



HAL
open science

OsFD4 promotes the rice floral transition via florigen activation complex formation in the shoot apical meristem

Martina Cerise, Francesca Giaume, Mary Galli, Bahman Khahani, Jérémy Lucas, Federico Podico, Elahe Tavakol, François Parcy, Andrea Gallavotti, Vittoria Brambilla, et al.

► To cite this version:

Martina Cerise, Francesca Giaume, Mary Galli, Bahman Khahani, Jérémy Lucas, et al.. OsFD4 promotes the rice floral transition via florigen activation complex formation in the shoot apical meristem. *New Phytologist*, 2021, 229 (1), pp.429-443. 10.1111/nph.16834 . hal-02953028

HAL Id: hal-02953028

<https://hal.science/hal-02953028v1>

Submitted on 1 Oct 2020

HAL is a multi-disciplinary open access archive for the deposit and dissemination of scientific research documents, whether they are published or not. The documents may come from teaching and research institutions in France or abroad, or from public or private research centers.

L'archive ouverte pluridisciplinaire **HAL**, est destinée au dépôt et à la diffusion de documents scientifiques de niveau recherche, publiés ou non, émanant des établissements d'enseignement et de recherche français ou étrangers, des laboratoires publics ou privés.



Distributed under a Creative Commons Attribution 4.0 International License

1 **OsFD4 promotes the rice floral transition via Florigen Activation Complex formation in the**
2 **shoot apical meristem**

3

4 Martina Cerise^{1,6}, Francesca Giaume¹, Mary Galli³, Bahman Khahani⁴, Jérémy Lucas⁵, Federico
5 Podico¹, Elahe Tavakol⁴, François Parcy⁵, Andrea Gallavotti³, Vittoria Brambilla² and Fabio
6 Fornara^{1,*}

7

8 ¹Department of Biosciences, University of Milan, Milan, 20123 Italy

9 ²Department of Agricultural and Environmental Sciences, University of Milan, Milan, 20123 Italy

10 ³Waksman Institute of Microbiology, Rutgers University, Piscataway, New Jersey, NJ 08854,
11 United States

12 ⁴Department of Crop Production and Plant Breeding, College of Agriculture, Shiraz University,
13 Shiraz, 71441-65186, Iran

14 ⁵University Grenoble Alpes, CNRS, CEA, INRAE, IRIG-DBSCI-LPCV, 17 avenue des martyrs, F-
15 38054, Grenoble, France

16 ⁶Max Planck Institute for Plant Breeding Research, Department of Developmental Biology,
17 Cologne, D-50829, Germany

18

19 *Correspondence: Fabio Fornara (fabio.fornara@unimi.it), Tel. +390250314817

20

21 Total word count: 6515

22 Introduction word count: 1163

23 Materials and Methods word count: 852

24 Results word count: 2628

25 Discussion word count: 1866

26 Number of figures: 6

27

28 Heading title: OsFD4 promotes flowering in rice

29

30 Associated twitter accounts: @fornaralab, @vittoriabr, @Francois_Parcy

31

32

33

34

35 **ORCID DETAILS**

36 Martina Cerise, <https://orcid.org/0000-0002-9654-252X>

37 Francesca Giaume, <https://orcid.org/0000-0002-6074-6950>

38 Bahman Khahani, <https://orcid.org/0000-0003-4499-2825>

39 Elahe Tavakol, <https://orcid.org/0000-0001-9033-7237>

40 François Percy, <https://orcid.org/0000-0003-2191-500X>

41 Andrea Gallavotti, <https://orcid.org/0000-0002-1901-2971>

42 Vittoria Brambilla, <https://orcid.org/0000-0003-0673-6898>

43 Fabio Fornara, <https://orcid.org/0000-0002-1050-0477>

44

45

46

47

48

49

50

51

52

53

54

55

56

57

58

59

60

61

62

63

64

65

66

67

68

69 **SUMMARY**

- 70 • In rice, the florigens Heading Date 3a (Hd3a) and Rice Flowering Locus T 1 (RFT1), OsFD-
71 like bZIP transcription factors, and Gf14 proteins assemble into Florigen
72 Activation/Repressor Complexes (FACs/FRCs), which regulate transition to flowering in
73 leaves and apical meristem. Only OsFD1 has been described as part of complexes promoting
74 flowering at the meristem, and little is known about the role of other bZIP transcription
75 factors, the combinatorial complexity of FAC formation, and their DNA binding properties.
- 76 • Here, we used mutant analysis, protein-protein interaction assays and DAP-sequencing
77 coupled to *in silico* prediction of binding syntaxes, to study several bZIP proteins that
78 assemble into FACs or FRCs.
- 79 • We identified OsFD4 as component of a FAC promoting flowering at the shoot apical
80 meristem, downstream of *OsFD1*. The *osfd4* mutants are late flowering and delay expression
81 of genes promoting inflorescence development. Protein-protein interactions indicate an
82 extensive network of contacts between several bZIPs and Gf14 proteins. Finally, we identified
83 genomic regions bound by bZIPs with promotive and repressive effects on flowering.
- 84 • We conclude that distinct bZIPs orchestrate floral induction at the meristem and that FAC
85 formation is largely combinatorial. While binding to the same consensus motif, their DNA
86 binding syntax is different, suggesting discriminatory functions.

87

88

89

90 Key words: bZIP, florigen activation complex, photoperiodic flowering, rice, shoot apical meristem.

91

92

93

94

95

96

97

98

99

100

101

102

103 INTRODUCTION

104 When external and internal conditions are favourable, plants switch their life cycle from the
105 vegetative to the reproductive phase. This process is called floral transition and is determined by
106 events taking place in both leaves and shoot apical meristem (SAM). In rice (*Oryza sativa*), transition
107 to the reproductive phase is controlled by changes in the photoperiod and is accelerated when day
108 length falls under a critical threshold. Because of this response, rice is classified as short day (SD)
109 plant. Yet, it can flower also under non-inductive long day (LD) conditions, after a prolonged
110 vegetative phase. As such, its photoperiodic response is facultative.

111 The molecular events that guide the floral transition start in the leaves when transcription of *Heading*
112 *date 3a (Hd3a)* and *RICE FLOWERING LOCUS T 1 (RFT1)* takes place in response to inductive
113 photoperiods. *Hd3a* and *RFT1* are homologs of Arabidopsis *FLOWERING LOCUS T (FT)* and
114 members of the phosphatidyl ethanolamine-binding protein (PEBP) family (Kojima *et al.*, 2002;
115 Komiya *et al.*, 2008, 2009). Similarly to *FT*, they are transcribed in companion cells of leaves;
116 subsequently, their cognate proteins can move through the phloem to reach the SAM, where they
117 promote expression of genes necessary to activate the inflorescence development program (Tamaki
118 *et al.*, 2007; Komiya *et al.*, 2009). Analysis of RNA interference lines and CRISPR mutants
119 demonstrated that a delay in flowering occurs upon downregulation of *Hd3a* or *RFT1* (Komiya *et al.*,
120 2008, Liu *et al.*, 2019). However, the phenotypic effects of reduced expression of *Hd3a* or *RFT1*
121 depend on the photoperiod. Under SD, *Hd3a* RNAi lines delay flowering and double *RFT1-Hd3a*
122 RNAi plants completely block it, indicating that both florigens can redundantly promote the floral
123 transition (Komiya *et al.*, 2008; Tamaki *et al.*, 2015). Conversely, *RFT1* RNAi lines delay flowering
124 under LD only, indicating that *RFT1* can promote flowering also under non-inductive photoperiods
125 (Komiya *et al.*, 2009). This difference correlates with the expression of *Hd3a* and *RFT1* in leaves:
126 when plants grow under SD conditions, both florigens are transcribed, whereas growth under non-
127 inductive LD conditions promotes *RFT1* expression only (Komiya *et al.*, 2008, 2009). Differential
128 sensitivity of *Hd3a* and *RFT1* transcription to day length is partly explained by distinct promoter
129 architectures (Komiya *et al.*, 2008, 2009).

130 Several positive and negative regulators control expression of the florigens in leaves. Among them,
131 the zinc finger transcription factor *Heading date 1 (Hd1)*, homolog of Arabidopsis CONSTANS,
132 promotes expression of *Hd3a* and *RFT1* under SD, while it represses it under LD (Yano *et al.*, 2000;
133 Hayama *et al.*, 2003). Hd1 functions as transcriptional regulator through physical interaction with
134 Grain yield, plant height and heading date 8 (Ghd8), Ghd7 and OsNF-YC7. Ghd8 and OsNF-YC7
135 are the B and C subunits of a heterotrimeric NF-Y complex, respectively, that assemble with Hd1,
136 bind the promoter of *Hd3a* and repress its transcription (Goretti *et al.*, 2017; Zhu *et al.*, 2017; Du *et*

137 *al.*, 2017). *Ghd7* encodes for a CCT domain protein that represses flowering (Xue *et al.*, 2008;
138 Nemoto *et al.*, 2016) .

139 The B-type response regulator *Early Heading date 1 (Ehd1)* is a major flowering promotor that shares
140 no homology with other genes of *Arabidopsis thaliana* (Doi *et al.*, 2004). *Ehd1* is expressed at higher
141 levels under SD conditions and preferentially promotes *Hd3a* transcription (Zhao *et al.*, 2015). In
142 agreement with its role as a flowering activator, *ehd1* mutants show a late flowering phenotype
143 compared to wild type, whereas *Ehd1* overexpression triggers early flowering under both SD and LD
144 conditions (Doi *et al.*, 2004; Itoh *et al.*, 2010; Cho *et al.*, 2016). Hd1 can repress *Ehd1* mRNA
145 expression under LD, by directly binding to its promoter (Nemoto *et al.*, 2016). These genetic
146 interactions are at the core of the photoperiodic flowering pathway in rice, which exhibits a different
147 architecture compared to the one of *Arabidopsis* (Andrés & Coupland, 2012).

148 When florigenic proteins are produced, they influence downstream gene expression by assembling
149 into Florigen Activation or Repressor Complexes (FACs/FRCs), higher-order complexes containing
150 PEBP molecules and FD-like bZIP transcription factors (Tsuji *et al.*, 2013; Brambilla *et al.*, 2017;
151 Kaneko-Suzuki *et al.*, 2018). The latter allow the complex to bind DNA at consensus sites
152 characterized by the core sequence ACGT (Izawa *et al.*, 1993). Interactions between florigens and
153 bZIPs can occur either directly or indirectly via bridging proteins called Gf14s, members of the 14-
154 3-3 protein family (Taoka *et al.*, 2011). In leaves, FACs/FRCs regulate expression of the florigens,
155 generating positive and negative feedback loops controlling *Ehd1* expression (Brambilla *et al.*, 2017).
156 More specifically, FRCs composed by the florigens and the bZIP transcription factor Hd3a BINDING
157 REPRESSOR FACTOR 1 (HBF1) delay the floral transition, as rice loss-of-function *HBF1* mutants
158 flower earlier compared to the wild type. HBF1 can bind the promoter of *Ehd1* to reduce its expression
159 in leaves, thus generating a negative feedback loop on *Hd3a* and *RFT1* production, that likely
160 modulates the amount of florigens being produced (Brambilla *et al.*, 2017).

161 Another bZIP transcription factor, *OsFD1*, encodes an interactor of the florigens and is part of a
162 flowering-promoting FAC (Taoka *et al.*, 2011). *OsFD1* is expressed in both leaves and SAM and
163 interacts with Hd3a and RFT1 only indirectly via Gf14 proteins. In leaves, *OsFD1* promotes the
164 expression of *Ehd1* generating a positive feedback loop on florigen production, whereas in the SAM,
165 *OsFD1*-containing FACs promote transcription of *OsMADS14* and *OsMADS15*, two key activators
166 of flower development in rice (Taoka *et al.*, 2011; Kobayashi *et al.*, 2012; Zhao *et al.*, 2015; Wu *et*
167 *al.*, 2017). Thus, the florigens not only connect leaves and SAM to convey seasonal information to
168 the apex, but their movement throughout the plant allows formation of distinct florigen-containing
169 complexes in different tissues and with diversified functions.

170 In the SAM, OsFD1 can further switch from activating to repressing flowering by forming FRCs. In
171 FRCs, OsFD1 interacts with four different CENTRORADIALIS-like proteins, *RICE*
172 *CENTRORADIALIS 1 (RCN1)*, *RCN2*, *RCN3* and *RCN4* which are PEBP and members of the TFL1-
173 like subclade (Kaneko-Suzuki *et al.*, 2018). They are expressed in the rice vascular tissue and,
174 similarly to Hd3a and RFT1, can move through the phloem and reach the SAM where they bind
175 OsFD1 via Gf14s, to regulate production of secondary branches of the panicle (Kaneko-Suzuki *et al.*,
176 2018).

177 Despite its central position in molecular complexes controlling flowering, *osfd1* RNA interference
178 plants showed almost no flowering delay compared to wild type plants (Taoka *et al.*, 2011). Its
179 interaction in both FACs and FRCs with opposite effects on flowering could partially explain such
180 phenotype. However, it cannot be excluded that additional bZIP transcription factors could operate
181 in parallel or redundantly with OsFD1.

182 Here, we functionally characterize *OsFD4*, an FD-like bZIP transcription factor promoting the floral
183 transition under both inductive and non-inductive photoperiodic conditions. We determine the extent
184 of OsFD4 interactions in FACs and its genetic relationship with OsFD1. Using Positional Weight
185 Matrices (PWM) gathered from DNA Affinity Purification sequencing (DAP-seq), we interrogate the
186 binding of OsFD1, OsDF4 and HBF1 to promoters of target genes, starting to define their distinct
187 modes of DNA binding.

188

189 **MATERIALS AND METHODS**

190 **Plant growth conditions, RNA preparation and quantification of gene expression**

191 The Nipponbare and Dongjin ecotypes (*Oryza sativa* L.) were used in this study. Plants were grown
192 in phytotrons under long-day conditions (14,5h light/9,5h dark) or short-day conditions (10h light/14h
193 dark). For quantification of gene expression using qRT-PCR, SAM samples were collected at
194 *Zeitgeber* (ZT) 0 in time courses of several days. Three biological replicates were performed for
195 *osfd4-1* time-courses. Two biological replicates were sampled for *osfd1-1* time courses. SAMs were
196 manually dissected under a stereomicroscope and the samples included the meristem proper as well
197 as some small meristematic leaves. For leaf samples, the distal part of mature leaves was used. RNA
198 was extracted with *TRIzol*® (Termofisher Scientific) following manufacturer's instructions. The
199 cDNA was retrotranscribed with Im-Prom-II RT (Promega) using a polyT primer and 1 µg of total
200 RNA as starting template. Quantification of transcripts was performed with the primers listed in Table
201 S1 using a RealPlex² thermocycler. The Maxima SYBR qPCR master mix (Termofisher Scientific)
202 was used in qRT-PCR experiments. Three technical replicates were performed for each qRT-PCR.

203

204 **Protein-protein interaction assays**

205 Yeast two hybrid was performed cloning the coding sequences into the vectors pGADT7 and
206 pGBKT7 (Clontech) and transformed into AH109 and Y187 yeast strains, respectively. Interactions
207 were tested by mating and growth on selective drop out media without the aminoacid -L-W-H-A
208 according to Brambilla et al., 2017.

209 BiFC experiments were performed using the vectors pBAT TL-B sYFP-N and pBAT TL-B sYFP-C.
210 Clones were transformed in tobacco epidermal cells by Agro-infiltration. Infiltrated leaves were
211 observed at the confocal 24 h after infiltration. Each interaction was tested in three different replicates.

212

213 **CRISPR-Cas9 cloning and Rice transformation**

214 The CRISPR-Cas9 vectors previously described by Miao et al., 2013 were used. We designed one
215 single-guide RNA for OsFD1, OsFD4 and OsFD3 (Table S1). We obtained edited *osfd4*, *osfd3* and
216 *osfd1* mutants starting from Nipponbare calli produced according to the protocol of Sahoo et al., 2011.
217 Rice calli were transformed using EHA105 *Agrobacterium tumefaciens* strain. Transformed calli
218 were selected on two selection media containing 50 mg/L and 100 mg/L of hygromycin, respectively.
219 After regeneration, we genotyped transformant plants via by sequencing PCR products amplified
220 across the single-guide RNA targeted region.

221

222 **DAP seq assay**

223 pENTR clones containing the *OsBZIP42*, *OsBZIP69*, and *OsBZIP77* ORFs were recombined into the
224 pIX-HALO vector and processed according to Bartlett et al., 2017. We used 1 ug of pIX-HALO-TF
225 plasmid DNA for protein expression in the TNT rabbit reticulocyte expression system (Promega).
226 For DNA binding reactions, 500 ng of adapter-ligated library prepared from genomic DNA extracted
227 from Nipponbare leaves was used. Libraries were sequenced on a NextSeq500 with 75bp single end
228 reads. A GST-HALO negative control sample was also processed in parallel and used for background
229 subtraction in peak calling.

230

231 **DAP-seq analysis**

232 Raw reads were trimmed using Trimmomatic (Bolger *et al.*, 2014) with the following parameters:
233 ILLUMINACLIP:TruSeq3-SE:2:30:10 LEADING:3 TRAILING:3 SLIDINGWINDOW:4:15
234 MINLEN:50. Trimmed reads were mapped to the *Osativa* v7 reference genome (release 40;
235 https://plants.ensembl.org/Oryza_sativa/) using Bowtie2 v2.2.8 (Langmead & Salzberg, 2012) with
236 default parameters. Mapped reads were filtered for reads aligning only to a single location in the
237 genome. Peaks were called using the GEM peak caller (Guo et al., 2012) as described in Galli et al.,

238 2018. PAVIS (Huang et al. 2013) was used to identify putative target genes. Target genes were
239 assigned based on the gene located closest to each peak and were restricted to those peaks located
240 5kb upstream of the TSS, 3kb downstream of the TES, or located within the gene. The 2000 interval
241 relative to the TSS was surveyed for detecting the position of peaks and distribution of them using a
242 bin size of 25 bp.

243 244 **Comparison between targets of *AtFD*, *OsFD1*, *OsFD4* and *OsHBF1***

245 In order to compare the FD-bound regions in *Arabidopsis* and rice, we retrieved ChIP-seq data for
246 FD from Collani et al. (2019). We next identified putative rice orthologs using the EnsemblPlants
247 (<https://plants.ensembl.org/index.html>) database (Table S2). The overlap between corresponding
248 genes bound by *AtFD*, *OsFD1*, *OsFD4* and *HBF1* was illustrated using a Venn diagram (Oliveros,
249 2007).

250 251 **Motif enrichment analysis and spacing/syntax analysis**

252 Peaks identified by the GEM (Guo et al., 2012) peak caller were used to compute motif enrichment,
253 using the MEME-suite (default arguments). Generated motifs were evaluated using ROC analysis to
254 estimate their prediction power, i.e. their capability to differentiate between bound and not bound
255 regions. For this, a negative set of non-bound regions with similar features (same length, same %GC,
256 same genomic origin [exonic, promoter,...] as the bound sequences) was generated as previously
257 described (Stigliani *et al.*, 2019). Detection of preferred spacings between motifs was done using the
258 called peaks and the MEME-generated position weight matrix (PWM). Predicted individual binding
259 sites were detected for a given threshold, for sets of both bound and unbound regions. Spacing
260 between predicted binding sites were computed for both sets. Enrichment was calculated by
261 comparing bound and not bound sets of regions. The PWM threshold values were empirically chosen:
262 we used a range of threshold values to ensure robustness of the result. Detailed methods are available
263 in Stigliani et al., 2019.

264 265 **RESULTS**

266 ***OsFD4* promotes flowering in rice**

267 In leaves, *HBF1*- and *OsFD1*-containing complexes control production of the florigens by regulating
268 *Ehd1* expression (Brambilla *et al.*, 2017). In the SAM, the *OsFD1*-containing FAC is known to
269 promote the floral transition by directly inducing expression of *OsMADS14* and *OsMADS15* (Taoka
270 *et al.*, 2011). Yet, *OsFD1* RNA interference plants showed only a marginally significant flowering
271 delay compared to the wild type, in sharp contrast to the phenotype shown by *Hd3a*-RNAi, *RFT1*-

272 RNAi and *Hd3a/RFT1* double RNAi plants (Komiya *et al.*, 2008). This suggests that other bZIP
273 transcription factors might share similar functions and compensate for reduced *OsFD1* expression.
274 We previously explored the bZIP family, searching for members having positive or negative effects
275 on the floral transition (Brambilla *et al.*, 2017). Here, we describe the functional characterization of
276 *bZIP69/OsFD4* (*LOC_Os08g43600*).

277 After searching the PFG rice T-DNA collection we identified line 2D_41663 in the Dongjin variety
278 that harboured a T-DNA insertion in the 3'-UTR of *OsFD4* (Fig. S1). The mutant line was renamed
279 *osfd4-1*. We could not detect *OsFD4* mRNA expression in *osfd4-1* (Fig. S1). Heading dates of the
280 mutant plants were assessed under both SD and LD, alongside Dongjin wild type controls. Mutant
281 plants flowered late under both conditions (Fig. 1a).

282 To validate the *osfd4-1* mutant phenotype, we generated additional *osfd4* mutant alleles using
283 CRISPR-Cas9 site-directed mutagenesis in the Nipponbare background (Miao *et al.*, 2013). We also
284 generated novel *osfd1* mutants to compare single mutant phenotypes. Finally, since we previously
285 showed that *OsFD4* strongly interacts with bZIP24/*OsFD3* (Brambilla *et al.*, 2017), we also generated
286 *osfd3* mutants (Fig. S1). Homozygous plants of the T1 generation were grown for two months under
287 non-inductive LD conditions and then shifted to inductive SD to score heading dates. As shown in
288 Fig. 1b and Fig. S1, *osfd4-3* showed delayed flowering compared to the wild type, confirming the
289 *osfd4-1* phenotype. The *osfd1-1* mutant flowered later than both wild type and *osfd4-3*, showing a
290 strong delay (Fig. 1b-d). The difference compared to published *OsFD1*-RNAi mutants could be due
291 to the different conditions used between studies, to the different genetic backgrounds used, or to a
292 limited reduction of *OsFD1* mRNA in RNAi lines. No effect on heading could be observed in *osfd3-*
293 *1* mutants (Fig. 1b).

294 To investigate the possible functional redundancy between *OsFD4* and *OsFD1*, we crossed *osfd4-1*
295 and *osfd1-2* mutants to generate an *osfd4-1 osfd1-2* double mutant (note that the genetic background
296 is mixed between Nipponbare and Dongjin). Flowering time experiments under inductive conditions
297 demonstrated that no additive effect could be detected in the *osfd4-1 osfd1-2* double mutant relative
298 to *osfd1-2* (Fig. 1d), i.e. the phenotypic effect observed was that of *osfd1-2* single (Fig. 1b-d). These
299 data indicate that *OsFD4* encodes a promotor of flowering in rice and that the effect of *osfd4* and
300 *osfd1* mutants is not additive.

301

302 ***OsFD4* is expressed in the shoot apical meristem and is regulated by *OsFD1***

303 *OsFD1* is expressed in both leaves and SAM. It promotes flowering, having distinct functions in both
304 tissues during the floral transition (Taoka *et al.*, 2011; Tamaki *et al.*, 2015; Jang *et al.*, 2017;
305 Brambilla *et al.*, 2017). We quantified the expression of *OsFD4* mRNA in leaves and apical

306 meristems, using qRT-PCR. Transcripts of *OsFD4* were detected in apical meristems but not in leaves
307 during the transition to flowering (Fig. 2a,b). Quantifications showed that *OsFD1* and *OsFD3*
308 expression was higher relative to *OsFD4* expression in both tissues.

309 To verify the epistatic interaction between *OsFD1* and *OsFD4*, observed in the *osfd4-1 osfd1-2*
310 double mutant, we analysed *OsFD4* and *OsFD1* mRNA levels in *osfd1-1* and *osfd4-1* mutants,
311 respectively. We observed that *OsFD4* expression was decreased in *osfd1-1* compared to the wild
312 type (Fig. 2c), whereas *OsFD1* expression was unchanged in *osfd4-1* mutants compared to wild
313 type (Fig. 2d). These data indicate that *OsFD1* is an upstream promoter of *OsFD4* expression, in
314 agreement with the phenotype of double *osfd4-1 osfd1-2* mutants (Fig. 1d).

315

316 **Network of interactions among FAC components**

317 The rice florigens interact with bZIP transcription factors either directly or through Gf14 proteins.
318 Interactions are likely dynamic and combinatorial, giving rise to several complexes, some also with
319 repressive functions (Zhao *et al.*, 2015; Jang *et al.*, 2017; Brambilla *et al.*, 2017; Kaneko-Suzuki *et*
320 *al.*, 2018). Dimers between Gf14 proteins form a W-shaped scaffold that bridges interactions with
321 bZIPs and with the florigens. We found that extensive combinatorial interactions are possible between
322 Gf14s expressed at the apex, giving rise to homo- and heterodimers (Fig. S2, all mating controls are
323 shown in Fig. S3). Interactions between Gf14s and bZIPs occur via the C-terminal SAP-domain,
324 which is common among several bZIPs, including OsFD4 and OsFD3 (Fig. S1). We tested whether
325 OsFD4 could interact with components of FACs. We first tested the binding between OsFD4 and the
326 six Gf14s expressed in the SAM, including Gf14A to Gf14F (Purwestri *et al.*, 2009). All six Gf14
327 proteins interacted with OsFD4 in Yeast-2-Hybrid (Y2H), but the strongest interactions were detected
328 between OsFD4 and Gf14A and Gf14F (Fig. 3a). Weaker yeast growth on -L-W-H-A selective media
329 was observed with other OsFD4-Gf14 combinations. Note that in a previous report we did not detect
330 the OsFD4-Gf14C interaction, using -L-W-H +3AT media (Brambilla *et al.*, 2017), consistent with
331 the findings of Kim *et al.*, 2016. Thus, interactions between OsFD4 and Gf14B, C, D, and E are likely
332 weak. Also, OsFD3 could interact with all Gf14s tested (Fig. S2).

333 We next asked if all Gf14 proteins expressed in the SAM could interact with RFT1 and Hd3a. Both
334 florigens interacted with all the Gf14s tested, suggesting that in the SAM, OsFD4, OsFD3 and OsFD1
335 can potentially form FACs indirectly via all 14-3-3 proteins (Fig. 3b). To confirm Y2H findings, we
336 performed BiFC with OsFD4 and Gf14B and observed reconstituted YFP expression in nuclei
337 indicating a positive interaction (Fig. S2).

338 Since HBF1 and HBF2 can directly contact Hd3a without the bridging function of Gf14s (Brambilla
339 *et al.*, 2017), we tested direct interactions between OsFD4 and Hd3a or RFT1. Using Y2H, we found

340 that OsFD4 can directly associate with RFT1, but no interaction was detected between OsFD4 and
341 Hd3a, whereas OsFD3 could interact with both florigens (Fig. 3c). These data are consistent with a
342 recent independent study, indicating that OsFD4 preferentially binds to one florigen only (Jang *et al.*,
343 2017). We then used BiFC to further test the OsFD4-RFT1 interaction, as well as to determine its
344 subcellular localization. We detected fluorescence in nuclei of *Nicotiana benthamiana* leaves
345 indicating nuclear localization of the heterodimer (Fig. 3d). No fluorescent signals could be detected
346 for the OsFD4–Hd3a interaction (Fig. 3e and Fig. S2).

347

348 **OsFD4 can homodimerize or heterodimerize with OsFD3**

349 bZIP transcription factors must homo- or heterodimerize to bind DNA (Dröge-Laser *et al.*, 2018).
350 We thus tested combinatorial interactions between bZIPs. We previously showed that OsFD4 and
351 OsFD3 can form homo- and heterodimers, whereas no dimerization was found with OsFD1
352 (Brambilla *et al.*, 2017; Fig. 3f,g). Here, we corroborated those results using BiFC, further showing
353 that OsFD4 and OsFD3 homo- and heterodimers are localized in the nucleus. We did not detect homo-
354 or heterodimerization of OsFD1 in BiFC assays (Fig. 3h,i).

355

356 **OsFD4 regulates expression of *API/FUL*-like genes**

357 The rice genome encodes four different *API/FUL*-like genes, *OsMADS14*, *OsMADS15*, *OsMADS18*
358 and *OsMADS20* which control flower development (Wu *et al.*, 2017). When plants are exposed to
359 inductive photoperiods and the meristem undergoes phase change, *OsMADS14*, *OsMADS15* and
360 *OsMADS18* increase their expression, whereas *OsMADS20* is downregulated (Kobayashi *et al.*, 2012;
361 Gómez-Ariza *et al.*, 2019). In the SAM, OsFD1 promotes the expression of *OsMADS14* and
362 *OsMADS15*. This regulation has been shown to be direct at least for *OsMADS15*, as the OsFD1-
363 containing FAC is able to bind to its promoter (Taoka *et al.*, 2011). To assess if an OsFD4-containing
364 FAC could also regulate the expression of *OsMADS* genes we measured transcription of *API/FUL*-
365 like genes in apical meristems of *osfd4-1*. We performed time course experiments shifting plants from
366 non-inductive LD conditions to inductive SD conditions and sampled SAMs at 0, 6, 12 and 18 Days
367 After Shifting (DAS). These time points were chosen based on the progression of floral transition in
368 rice which becomes irreversible at 12 SDs, after which a fully committed SAM develops into a
369 branched inflorescence (Kobayashi *et al.*, 2012; Gómez-Ariza *et al.*, 2019). Comparing *OsMADS*
370 gene expression between wild type Dongjin and *osfd4-1* plants, we observed that *OsMADS14* and
371 *OsMADS15* levels could increase in the mutant but at slower rates, whereas expression of *OsMADS18*
372 and *OsMADS20* was not changed compared to the wild type (Fig. 4a-d).

373 Rice *API/FUL*-like genes work together with *OsMADS34/PAP2*, a *SEPALLATA (SEP)*-like gene, to
374 promote the floral transition (Kobayashi *et al.*, 2010, 2012). Expression of *OsMADS34/PAP2*
375 increased in both wild type and *osfd4-1* but was significantly delayed in the mutant (Fig. 4e). To
376 complete our analysis, we also quantified the expression of *API/FUL*-like genes and of
377 *OsMADS34/PAP2* in the *osfd1-1* mutant. We observed that their expression had similar dynamics in
378 both *osfd1-1* and *osfd4-1* (Fig. 4f-j). Taken together, these data suggest that OsFD4-FAC, as well as
379 OsFD1-FAC, act upstream of *OsMADS* genes to promote the rice floral transition.

380

381 **Genome-wide identification of OsFD4, OsFD1 and HBF1 binding sites**

382 In the SAM, changes in the photoperiod regulate the transcription of several genes (Furutani *et al.*,
383 2006; Kobayashi *et al.*, 2012; Tamaki *et al.*, 2015; Gómez-Ariza *et al.*, 2019). Yet, only a few genes
384 are known to be under control of FACs/FRCs. As a first screen to identify DNA binding sites of bZIP
385 transcription factors and FAC-regulated genes, we performed DNA Affinity Purification sequencing
386 (DAP-seq) using OsFD4, OsFD1 and HBF1 (O'Malley *et al.*, 2016; Bartlett *et al.*, 2017; Galli *et al.*,
387 2018). Peak calling analysis identified 1107 DAP-peaks for OsFD4, 2059 DAP-peaks for OsFD1,
388 and 28323 DAP-peaks for HBF1 (Fig. 5a). The top enriched motif for OsFD1, OsFD4 and HBF1
389 contained the core consensus motif CACGT, the known binding site for many bZIP transcription
390 factors known as G-box (Fig. 5a) (O'Malley *et al.*, 2016). At the flanks of this core motif, two
391 nucleotides -GC- were enriched with different frequencies, depending on the bZIP tested. For
392 example, OsFD4 peaks were most enriched for the motif GCCACGT (Fig. 5a).

393 To identify putative target genes regulated by these binding events, we assigned all DAP-peaks lying
394 within 5000 bp upstream of an ATG and 3000 bp downstream of a STOP codon (including regions
395 within exons and introns) to the closest gene. Based on this analysis, HBF1 peaks were associated
396 with 15,937 putative target genes, and OsFD1 and OsFD4 were associated with 1,717 and 925
397 putative target genes, respectively (Fig. 5a; Table S3). Most of the binding sites fell in putative
398 promoter regions (Fig. 5b). The highest frequency of peaks (30% for OsFD4, 27% for OsFD1 and
399 17% for HBF1) was in the 500 bp upstream of the transcription start site (TSS; Fig. 5c), consistent
400 with these sites being highly represented in the core promoter sequences. We next examined the
401 overlap between genes bound by OsFD1, OsFD4 and HBF1 and observed that 698 putative target
402 genes were shared by all tested bZIPs; 220 genes were shared by OsFD4 and HBF1, and 991 were
403 shared by OsFD1 and HBF1. All genes common to OsFD1 and OsFD4 were also common to HBF1,
404 thus no gene was found at the intersection between OsFD1 and OsFD4 datasets only (Fig. 5d and
405 Table S3). Finally, 7, 28 and 14,028 genes were uniquely targeted by OsFD4, OsFD1 or HBF1 (Fig.
406 5d).

407 The DAP-seq method uses the entire naked genome to identify transcription factor binding sites.
408 Thus, many bound regions might not be functionally relevant for regulation of gene expression *in*
409 *vivo* (O'Malley *et al.*, 2016; Bartlett *et al.*, 2017). To focus our analysis on those tissues where OsFD4,
410 OsFD1 and HBF1 are expressed (Fig. 2a), we filtered for genes expressed specifically in the SAM
411 and mature leaves. To this end, we first compared the lists of genes bound by OsFD1 and OsFD4 to
412 those expressed in the shoot apex, based on recently published RNA-seq data (Fig. 5e) (Gómez-Ariza
413 *et al.*, 2019). The lists of genes bound by HBF1 and OsFD1 were compared to the list of genes
414 expressed in mature leaves, again as determined by published RNA-seq data (Galbiati *et al.*, 2016)
415 (Fig. 5f). This analysis identified 240 genes expressed in shoot apices that were putative targets of
416 both OsFD4 and OsFD1, 58 genes that were putative targets of OsFD4, and 320 genes that were
417 putative targets of OsFD1 (Fig. 5e). Of those genes showing expression in mature leaves, 566 were
418 putative targets of both HBF1 and OsFD1, 3691 were putative targets of HBF1, and seven were
419 putative targets of OsFD1 (Fig. 5f).

420 Finally, we compared putative targets of OsFD1, OsFD4 and HBF1 with targets of AtFD (Collani *et*
421 *al.*, 2019). To this end, genes identified by ChIP-seq data were retrieved from Collani *et al.* (2019)
422 and the corresponding putative rice orthologs were assigned based on the EnsemblPlants database
423 (Table S2). The overlap between corresponding genes indicates the existence of targets possibly being
424 part of common regulatory modules, evolutionary conserved (Fig. S4 and Table S4).

425

426 ***OsMADS62* and *OsARF19* are targets of both the *OsFD4*-FAC and *OsFD1*-FAC**

427 To determine if binding of OsFD1 and OsFD4 to genomic regions correlated with transcriptional
428 regulation of the neighboring genes, we quantified transcript abundance of selected target genes in
429 *osfd1-1*, *osfd4-1* and wild type. For this analysis, we focused on several transcription factors
430 expressed in the apical meristem and whose promoters contained OsFD1 or OsFD4 binding peaks.
431 These included two genes bound by both *OsFD1* and *OsFD4*, *LOC_Os08g38590* (*OsMADS62*) and
432 *LOC_Os06g48950* (*OsARF19*), three genes bound only by *OsFD1*, *LOC_Os01g14440* (*WRKY*),
433 *LOC_Os01g64360* (*MYB*), and *LOC_Os04g51000* (*RICE FLORICAULA/LEAFY*), and two genes
434 bound by *OsFD4* only, *LOC_Os04g31730* (*B3*) and *LOC_Os07g41580* (*NF-YB*) (Fig. 5g-h and Fig.
435 S5). Expression of both *OsMADS62* and *OsARF19* was reduced in *osfd4-1* and *osfd1-1* compared to
436 the wild type, suggesting that OsFD1 and OsFD4 may be direct activators of both genes (Fig. 5g-h).
437 The other genes tested showed reduced expression in both mutants relative to wild type probably
438 because of the epistatic effect of *OsFD1* to *OsFD4* (Fig. S5). These data suggest that OsFD4 and
439 OsFD1 regulate several common target genes, but their transcriptional effects are not completely
440 overlapping.

441

442 **OsFD4, OsFD1 and HBF1 show preferential DNA binding configurations**

443 OsFD1, OsFD4 and HBF1 bind overlapping but also distinct sets of genes in DAP-Seq experiments,
444 yet they recognize a very similar motif. Because bZIP TFs are known to bind to tandem motifs, we
445 asked if spacing between CACGT consensus motifs found in OsFD1, OsFD4 and HBF1 DAP-seq
446 peaks varied. We used a Position Weight Matrix (PWM) derived from DAP-seq data to locate bZIP
447 binding sites and test whether there are some preferences in terms of binding syntaxes (spacing and
448 configuration between two consensus motifs (Fig. 6a) (Stigliani *et al.*, 2019). We first evaluated the
449 predictive power of the generated PWM which resulted exceptionally high, with ROC values of
450 0.985, 0.971 and 0.9 respectively (Fig. S6). Next, we analyzed the distribution of spacings for each
451 bZIP, quantifying overrepresented configurations against a set of negative regions (unbound), and we
452 found specific profiles for each bZIP.

453 Direct Repeats (DR) 0, Everted Repeats (ER) 1, 5, ER18-20, ER44, Inverted Repeats (IR) 41
454 configurations showed at least a 4-fold overrepresentation among OsFD4 bound regions, with the
455 ER44 configuration being highly overrepresented (Fig. 6b). Regions bound by OsFD1 showed a
456 robust enrichment of at least 3-fold in the DR30, ER4, ER16, ER32-34, ER41-2 and ER46, and IR38
457 configurations (Fig. 6c), with ER16 and ER32-34 as the most overrepresented. Configuration
458 enrichments for HBF1 included DR29, DR40, ER3, ER16-18, ER42 and IR10 with at least 2-fold
459 enrichment compared to the negative set of regions (Fig. 6d). These data identify different spacing
460 configurations between consensus motifs, which are preferred by OsFD4, OsFD1 and HBF1 and
461 likely contribute to the specificity of target recognition.

462

463 **DISCUSSION**

464 Transcription factors of the bZIP family have important roles during phase transitions in different
465 plant species (Abe *et al.*, 2005; Wigge *et al.*, 2005; Taoka *et al.*, 2011; Tsuji *et al.*, 2013; Park *et al.*,
466 2014; Tylewicz *et al.*, 2015; Brambilla *et al.*, 2017; Teo *et al.*, 2017). However, those controlling
467 flowering time and for which functional studies have been carried out, appear insufficient to account
468 for all aspects of phase change, suggesting a certain level of redundancy, or the existence of additional
469 transcriptional regulators. In rice, the role of OsFD1 as a promoter of flowering has been supported
470 by overexpression studies, but the analysis of RNAi mutants failed to demonstrate phenotypic effects
471 on flowering (Taoka *et al.*, 2011; Jang *et al.*, 2017; Brambilla *et al.*, 2017). Other *OsFD*-like genes
472 have been investigated previously, however they perform functions distinct from those of OsFD1
473 (Tsuji *et al.*, 2013; Brambilla *et al.*, 2017). Here, to identify additional components of florigen
474 signalling, we reported the characterization of OsFD4 and OsFD3, as well as further insights into

475 OsFD1 function based on CRISPR-mediated mutagenesis. While describing such additional FD-like
476 components integrating florigen signalling, it became clear that despite similar modes of action,
477 differences in their expression profiles, specific combinatorial interactions with Gf14 proteins and
478 florigens, and distinct DNA binding syntaxes distinguish different members of the family.

479

480 **The FAC paradigm across Angiosperms**

481 Formation of a FAC requires that florigenic proteins that have reached the SAM first interact in the
482 cytosol with Gf14 proteins and then enter the nucleus, where phosphorylated bZIP transcription
483 factors contact the Gf14 and contribute a DNA-recognition function. This model of interaction
484 between florigens and bZIP transcription factors was first proposed in Arabidopsis and later supported
485 by studies in rice, where the role of Gf14s as bridges was identified. Subsequently, it has been
486 extended to many other species including dicots and monocots and shown to control a wide range of
487 developmental processes.

488 In rice, the functional homolog of Arabidopsis FD is encoded by *OsFD1*. When overexpressed using
489 either a constitutive or phloem-specific promoter, *OsFD1* can accelerate flowering (Jang et al., 2017,
490 Brambilla et al., 2017). However, RNAi lines flower similarly to wild type, possibly *OsFD1*
491 transcripts are not completely absent in these knock-down lines (Taoka *et al.*, 2011). Thus, the
492 functional significance of OsFD1 as a flowering regulator has remained unclear. Knock-out of *OsFD1*
493 using CRISPR-Cas9 showed that the gene has indeed a prominent effect in promoting flowering. This
494 is likely the result of a more complex molecular function that includes (i) induction of *OsMADS14*
495 and *15* gene expression in the SAM and in leaves, (ii) induction of *Ehd1*, *Hd3a* and *RFT1* mRNA
496 expression in leaves, and (iii) interaction with RCNs in repressor complexes that antagonize FAC-
497 dependent activation of *OsMADS* gene expression. Thus, OsFD1 and Gf14 proteins are central to
498 both activating and repressive flowering pathways, the switch between them being likely controlled
499 by the relative abundance of FT-like and TFL1-like proteins at the apex.

500 Still, while double *Hd3a* and *RFT1* RNAi mutants do not flower for up to 300 days under inductive
501 SDs, single *osfd1* loss-of-function mutants are delayed in flowering but they can flower, an apparent
502 inconsistency justified by functional redundancy between bZIPs (Komiya *et al.*, 2008). In
503 Arabidopsis, FD is redundant with FD PARALOG (FDP). Double *fd fdp* mutations flower later than
504 *fd* single, and almost completely suppress precocious flowering of *35S:FT* (Jaeger *et al.*, 2013). In
505 rice, by mutating additional bZIPs, including *OsFD3* and *OsFD4*, we have identified floral promoting
506 factors. Mutations in *osfd4*, but not in *osfd3*, can delay flowering and activation of *OsMADS* targets.
507 However, flowering was not delayed as much as in *osfd1* mutants, indicating a less prominent role
508 compared to OsFD1. Also, *osfd1 osfd4* double mutants did not further delay flowering compared to

509 *osfd1* single mutants. Based on expression data, we propose that *OsFD1* activates *OsFD4*
510 transcription. Thus, in *osfd1* mutants, the levels of both regulators are low. This arrangement does not
511 fully exclude redundancy but suggests a complex regulatory network.

512 Considering the interaction patterns with the florigens, we found that OsFD4 can interact directly
513 with RFT1, but only via Gf14s with Hd3a, suggesting different preferences for FAC architectures.
514 The SAM of rice is induced to flower by both florigens under SD, but only by RFT1 under LD
515 (Komiya *et al.*, 2008, 2009). Since the flowering delay observed in *osfd4* mutants is much stronger
516 under LD than under SD, we propose that different bZIPs perform distinct functions in the
517 photoperiod, and that the OsFD4-RFT1 module is key to promote flowering mostly under non-
518 inductive conditions.

519

520 **DAP-Seq identifies genome-wide OsFD1, OsFD4 and HBF1 binding sites**

521 Application of DAP-seq using purified OsFD1, OsFD4 and HBF1 proteins resulted in the
522 identification of hundreds of putative direct binding sites for these bZIPs. Consistent with a function
523 in core promoters, binding sites were enriched in the proximity of the TSS. It should be noted that the
524 *in vitro* nature of DAP-seq allows for the identification of direct binding events by a single TF,
525 specifically capturing those mediated by individual homodimers. Given that OsFD1, OsFD4 and
526 HBF1 formed heterodimers, these events may represent only a fraction of all *in vivo* binding events
527 resulting from additional protein interactions. Integrating DAP-seq data with expression data allowed
528 us to focus specifically on those genes that were expressed in relevant tissues and on those
529 differentially expressed in the *osfd4-1* and *osfd1-2* mutants. Our data provide a first examination of
530 the direct genome-wide binding landscape of bZIP flowering regulators in rice. This approach needs
531 now to be refined for several reasons.

532 First, we used a single purified bZIP transcription factor in DAP-seq reactions. Being disengaged
533 from its florigen-containing complex, its DNA binding capacity might be biased. Arabidopsis FD can
534 bind functional sites without assembling into a FAC and with no need for FT or its closest homologue,
535 TWIN SISTER OF FT (TSF) (Collani *et al.*, 2019). Also purified OsFD1 alone can bind a fragment
536 of the *AP1* promoter containing a C-box element (GACGTC) in gel shift assays (Taoka *et al.*, 2011).
537 We previously showed that HBF1 can bind *in vitro* an ABRE/G-box element in the *Ehd1* promoter
538 region, a finding that we further corroborated in this study (Brambilla *et al.*, 2017). Thus, bZIPs are
539 likely to conserve their basal DNA binding ability even when not combined in ternary complexes,
540 but despite these examples, affinity for DNA is likely potentiated by binding with other interactors,
541 including members of the PEBP family (Collani *et al.*, 2019).

542 Second, since bZIPs bind the DNA as homo or heterodimers, and given their combinatorial
543 interactions and overlapping expression in different plant tissues, including the SAM, it cannot be
544 excluded that DNA binding specificity changes when assessing heterodimeric configurations.

545 Third, bZIPs might be incorporated into higher order complexes that include other transcriptional
546 regulators with different DNA binding properties. In Arabidopsis, SQUAMOSA PROMOTER-
547 BINDING PROTEIN-LIKE 3 (SPL3), SPL4 and SPL5 interact with FD to enhance its transcriptional
548 activation of target genes and its specificity for target promoters (Jung *et al.*, 2016). Since SPLs are
549 produced at the SAM in response to plant aging, the SPL-FD complex has been proposed to integrate
550 photoperiodic and aging signals to activate the *API* promoter (Jung *et al.*, 2016). The study further
551 suggested that the proximal C-box in the *API* promoter is dispensable for FD-mediated induction,
552 and that a distinct SPL-binding site might contribute to transcription of *API*. A similar case has been
553 described for Class II TCP transcription factors, including TCP5, 13 and 17. These proteins can
554 physically interact with FD, and facilitate its binding to the *API* promoter. Also in this case, binding
555 of FD to the *API* promoter was not observed at the C-box, but was dependent upon a TCP binding
556 motif located between the SPL-binding site and the C-box (Li *et al.*, 2019).

557 Finally, post transcriptional modifications have a major role *in vivo*. Many FD-like proteins harbour
558 at their C terminus an SAP domain containing serine, threonine or both, which needs to be
559 phosphorylated to interact with Gf14s (Taoka *et al.*, 2011; Park *et al.*, 2014; Li *et al.*, 2015; Collani
560 *et al.*, 2019). When phosphorylated, Arabidopsis FD has a higher affinity for DNA. Expression of
561 phosphomimic versions of FD or OsFD1 can accelerate flowering in Arabidopsis and rice,
562 respectively. The kinases responsible for phosphorylation in Arabidopsis include Calcium-dependent
563 Protein Kinase 6 (CPK6) and CPK33, which interact with FD and, if mutated, slightly delay flowering
564 (Kawamoto *et al.*, 2015). Thus, optimal DNA binding and floral promoting activity of FAC
565 complexes likely relies on this modification of the bZIP components. Future DNA-binding
566 experiments either *in vivo* or using multiple complex components could help elucidate the individual
567 contributions of each component.

568 569 **Direct targets of OsFD1 and OsFD4 and alternative binding syntaxes**

570 Despite these caveats, DAP-seq led to the identification of several putative direct targets of the bZIPs
571 studied here, out of which *OsmADS62* and *ARF19* were validated as transcriptionally regulated by
572 both OsFD1 and OsFD4. *OsmADS62* controls pollen maturation and germination, partially
573 redundantly with *OsmADS63* and *OsmADS68* (Liu *et al.*, 2013). OsFD1 and OsFD4 promoted
574 *OsmADS62* expression, a function they likely perform after meristem commitment, during
575 inflorescence and flower development. *OsARF19* encodes for an AUXIN RESPONSE FACTOR

576 broadly expressed in the plant but with higher levels of transcription in the shoot, which is further
577 elevated by auxin treatments (Zhang et al., 2015).

578 We did not find OsFD1 or OsFD4 bound to the *OsMADS14*, *OsMADS15* or *OsMADS34/PAP2*
579 promoter. *OsMADS15* has been proposed as direct target of an OsFD1-containing FAC (Taoka et al.,
580 2011). Other proteins could possibly stabilize OsFD4 and OsFD1 *in vivo* and allow binding to these
581 *loci*. Alternatively, the rice OsFD1-*OsMADS* connection might be indirect. Data in support of a direct
582 connection have not been as thoroughly repeated and validated in rice as they have been in
583 *Arabidopsis*, in which direct contacts between FD and the C-box element in the *API* promoter were
584 disproved (Benlloch et al., 2011; Jung et al., 2016; Collani et al., 2019; Li et al., 2019). Further
585 assessment of *in vivo* binding will be necessary.

586 Genome scanning by DAP-seq identified identical core bZIP-binding motifs that were highly
587 enriched in peaks of all three bZIP datasets. The same 5'-CACGT-3' core motif was identified as
588 bound by OsFD1, OsFD4 and HBF1. The same 5'-CACGT-3' core motif was identified as enriched
589 among FD binding regions *in vivo*, suggesting conservation between rice and *Arabidopsis*, and indeed
590 many other bZIPs from diverse organisms (Dröge-Laser et al., 2018).

591 We found that despite identical core DNA binding sites, spacing among tandem motifs was different
592 for each of the three bZIPs tested in our assay. OsFD1 and OsFD4 which are activators of the rice
593 floral transition prefer to bind the DNA with ER conformations, whereas HBF1, a repressor, binds
594 more frequently ER and DR conformations. These results indicate distinct and specific binding
595 syntaxes for each transcription factor. The method was recently applied to define binding syntaxes of
596 MONOPTEROS (MP) and AtARF2, which have opposing transcriptional functions but share the
597 same consensus motif (Stigliani et al., 2019). The method can capture DNA binding features of
598 proteins that interact as either homo or heterodimers, but the ER or DR arrangements might suggest
599 the possibility of more elaborated structures, including tetramers.

600 **FIGURE LEGENDS**

601

602 **Figure 1. The *osfd4* and *osfd1* mutants delay rice flowering.**

603 (a) Days to heading of *Dongjin* wild type (Dj) and *osfd4-1* under inductive short day conditions (SD)
604 and non-inductive long day conditions (LD). (b) Days to heading of *Nipponbare* wild type (Nb),
605 *osfd1-1*, *osfd3-1* and *osfd4-3* under SD conditions. (c) Representative pictures of *osfd1-1* (left) and
606 Nb (right) plants. White arrows indicate emerging panicles. (d) Days to heading of Nb, *osfd1-2*, Dj,
607 *osfd4-1* and double *osfd4-1 osfd1-2* mutants under SD conditions. Data are represented as mean \pm
608 StDev. Asterisks indicate the p-value calculated using ANOVA, ****= $p < 0.0001$, **= $p < 0.01$, ns=non
609 significant. All flowering time experiments were repeated at least twice, and one representative
610 experiment is shown in (a) and (b). The graph in (d) includes data from three independent
611 experiments.

612

613 **Figure 2. Temporal expression pattern of *OsFD1*, *OsFD3* and *OsFD4* in the shoot apical
614 meristem of rice and genetic interaction between *OsFD1* and *OsFD4*.**

615 Quantification of *OsFD1*, *OsFD3* and *OsFD4* transcripts in the SAM (a) and in leaves (b) of Nb wild
616 type. DAS, Days After Shift from long day (LD) to short day (SD) conditions. (c) Quantification of
617 *OsFD4* transcripts in SAMs of *osfd1-1* mutants. (d) Quantification of *OsFD1* transcripts in SAMs of
618 *osfd4-1* mutants. Each time point represents the mean \pm StDev of three technical replicates. The
619 experiments were repeated twice with similar results. Ubiquitin was used to normalize gene
620 expression.

621

622 **Figure 3. Interactions between OsFD1, OsFD3, OsFD4 and components of Florigen Activation
623 Complexes (FACs) determined in yeast and tobacco.**

624 (a) Interactions between Activation Domain (AD)-OsFD1, AD-OsFD4 and Binding Domain (BD)-
625 Gf14A-F. (b) Interactions between AD-Gf14A-F and BD-Hd3a and BD-RFT1. (c) Interactions
626 between AD-OsFD4, AD-OsFD3 and Hd3a and RFT1 fused to the BD. Bimolecular fluorescence
627 complementation (BiFC) between OsFD4 fused with N-terminus of YFP (N-YFP) and (d) RFT1
628 fused with the C-terminus of YFP (C-YFP) or (e) Hd3a fused with the C-YFP. (f) Interactions
629 between OsFD4 and OsFD1 fused with the AD or the BD. (g) Interactions between OsFD3, OsFD4
630 and OsFD1 fused to the BD and OsFD3 fused to the AD. (h) Assessment of OsFDs homodimerization
631 by BiFC. From left, OsFD4:N-YFP/OsFD4:C-YFP, OsFD1:N-YFP/OsFD1:C-YFP and OsFD3:N-
632 YFP/OsFD3:C-YFP. (i) Assessment of OsFDs heterodimerization by BiFC. From left OsFD4:N-
633 YFP/OsFD1:C-YFP, OsFD3:N-YFP/OsFD4:C-YFP and OsFD1:N-YFP/OsFD3:C-YFP.

634 Interactions were determined in yeast on selective drop out media -L-W-H-A. The yeast experiments
635 were repeated three times with identical results. AD and BD clones containing empty vectors were
636 used as negative controls. BiFC experiments were repeated three times in tobacco with identical
637 results. N-YFP and C-YFP clones containing empty vectors were used as negative controls. DAPI
638 stain was used to mark nuclei.

639

640 **Figure 4. *OsFD4* and *OsFD1* promote *OsMADS14* and *15* transcription in rice.**

641 Quantification of (a), (f) *OsMADS14*, (b), (g) *OsMADS15*, (c), (h) *OsMADS18*, (d), (i) *OsMADS20*,
642 and (e), (j) *OsMADS34/PAP2* transcription in *Dongjin* vs. *osfd4-1* mutants (a)-(e) and in *Nipponbare*
643 vs. *osfd1-1* mutants (f)-(j). Expression was quantified in plants grown for two months under long day
644 (LD) and then shifted to short day (SD) conditions. Apical meristems were sampled at 0, 6, 12 and
645 18 Days After Shifting (DAS).

646

647 **Figure 5. Identification of *OsFD1*, *OsFD4* and *HBF1* binding sites.**

648 (a) Summary of DNA Affinity Purification sequencing (DAP-seq) results of *OsFD1*, *OsFD4* and
649 *HBF1*, including number of peaks, putative target genes and consensus motives. (b) Distribution of
650 peaks within gene features. (c) Distribution of peaks near the Transcriptional Start Site (TSS) of
651 putative target genes. (d) Venn diagrams showing the overlap between putative target genes of
652 *OsFD1*, *OsFD4* and *HBF1*. (e) Venn diagrams showing the overlap between targets of *OsFD1* and
653 *OsFD4* and genes expressed at the apical meristem. (f) Venn diagrams showing the overlap between
654 targets of *OsFD1* and *HBF1* and genes expressed in leaves. Genome browser view of *OsFD1* and
655 *OsFD4* binding peaks in the 3'UTR of *OsMADS62* (g) and in the putative promoter of *OsARF19* (h),
656 and quantification of transcripts in *osfd4-1* and *osfd1-1* mutants. Black arrows indicate the direction
657 of transcription. Asterisks indicate $p < 0.01$ (*), $p < 0.005$ (**), $p < 0.001$ (***), $p < 0.0001$ (****) based
658 on Student's t test, ns=non significant. Each time point represents the mean \pm St Dev of three technical
659 replicates. The experiments were repeated twice with similar results. Ubiquitin was used to normalize
660 gene expression.

661

662 **Figure 6. Analysis of *OsFD1*, *OsFD4* and *HBF1* binding syntax.**

663 (a) Scheme of Everted Repeats (ER), Direct Repeats (DR) and Inverted Repeats (IR) of "ACGTGGC"
664 motives. Blue and green arrows represent the first and the second binding motifs. N=general base;
665 n=number of base pairs between the two motifs. (b)-(d) Spacing analysis of absolute and normalized
666 enrichment of *OsFD4* (b), *OsFD1* (c) and *HBF1* (d) binding sites. The numbers on top of the graphs
667 represent the distance between two consensus motives.

668

669 **Supplemental figures and tables**

670 **Fig. S1** Genotype and phenotype of *OsFD4* and *OsFD1* mutants

671 **Fig. S2** OsFD3 and Gf14s Y2H assays and OsFD4-Hd3a BiFC

672 **Fig. S3** Y2H mating controls

673 **Fig. S4** Venn diagram showing the overlap between targets of AtFD, OsFD1, OsFD4 and HBF1

674 **Fig. S5** Expression analysis of some DAP-seq targets in *osfd4-1* and *osfd1-1*

675 **Fig. S6** Spacing analysis control: OsFD4, OsFD1 and HBF1 ROC curves

676 **Table S1** Sequences of oligonucleotides used in this study

677 **Table S2** Arabidopsis orthologs of rice genes

678 **Table S3** List of OsFD4, OsFD1 and HBF1 DAP-seq bound genes

679 **Table S4** List of genes shown in Figure S4

680

681 **Acknowledgements**

682 The authors wish to thank the NOLIMITS microscopy facility and Botanical Garden Città Studi for
683 technical support. This work was supported by an ERC Starting Grant (#260963) and PRIN
684 (#20153NM8RM) to FF.

685

686 **Author Contributions**

687 MC, MG, JL, F Parcy, AG, VB and FF designed research; MC, FG, MG, BK, JL and F Podico
688 performed research; MC, FG, MG, BK, JL, ET, VB and FF analysed and interpreted data; MC and
689 FF wrote the manuscript.

690

691 **REFERENCES**

692 **Abe M, Kobayashi Y, Yamamoto S, Daimon Y, Yamaguchi A, Ikeda Y, Ichinoki H, Notaguchi**
693 **M, Goto K, Araki T. 2005.** FD, a bZIP Protein Mediating Signals from the Floral Pathway
694 Integrator FT at the Shoot Apex. *Science* **309**: 1052–1056.

695 **Andrés F, Coupland G. 2012.** The genetic basis of flowering responses to seasonal cues. *Nature*
696 *Reviews. Genetics* **13**: 627–39.

697 **Bartlett A, Malley RCO, Huang SC, Galli M, Nery JR, Gallavotti A, Ecker JR. 2017.** Mapping
698 genome-wide transcription-factor binding sites using DAP-seq. *Nature Protocols* **12**: 1659–1672.

699 **Benlloch R, Kim MC, Sayou C, Thévenon E, Parcy F, Nilsson O. 2011.** Integrating long-day

700 flowering signals: a LEAFY binding site is essential for proper photoperiodic activation of
701 *APETALA1*. *The Plant Journal* **67**: 1094–1102.

702 **Bolger AM, Lohse M, Usadel B. 2014.** Genome analysis Trimmomatic: a flexible trimmer for
703 Illumina sequence data. *Bioinformatics* **30**: 2114–2120.

704 **Brambilla V, Martignago D, Goretti D, Cerise M, Somssich M, de Rosa M, Galbiati F,**
705 **Shrestha R, Lazzaro F, Simon R, et al. 2017.** Antagonistic Transcription Factor Complexes
706 Modulate the Floral Transition in Rice. *The Plant Cell* **29**: 2801–2816.

707 **Cho L-H, Yoon J, Pasriga R, An G. 2016.** Homodimerization of Ehd1 Is Required to Induce
708 Flowering in Rice. *Plant Physiology* **170**: 2159–2171.

709 **Collani S, Neumann M, Yant L, Schmid M. 2019.** FT Modulates Genome-Wide DNA-Binding of
710 the bZIP Transcription Factor FD. *Plant Physiology* **180**: 367–380.

711 **Doi K, Izawa T, Fuse T, Yamanouchi U, Kubo T, Shimatani Z, Yano M, Yoshimura A. 2004.**
712 *Ehd1*, a B-type response regulator in rice, confers short-day promotion of flowering and controls
713 *FT*-like gene expression independently of *Hd1*. *Genes & Development* **18**: 926–36.

714 **Dröge-Laser W, Snoek BL, Snel B, Weiste C. 2018.** The Arabidopsis bZIP transcription factor
715 family — an update. *Current Opinion in Plant Biology* **45**: 36–49.

716 **Du A, Tian W, Wei M, Yan W, He H, Zhou D, Huang X, Li S, Ouyang X. 2017.** The DTH8-
717 Hd1 Module Mediates Day-Length-Dependent Regulation of Rice Flowering. *Molecular Plant* **10**:
718 948–961.

719 **Furutani I, Sukegawa S, Kyojuka J. 2006.** Genome-wide analysis of spatial and temporal gene
720 expression in rice panicle development. *The Plant Journal* **46**: 503–11.

721 **Galbiati F, Chiozzotto R, Locatelli F, Spada A, Genga A, Fornara F. 2016.** *Hd3a*, *RFT1* and
722 *Ehd1* integrate photoperiodic and drought stress signals to delay the floral transition in rice. *Plant,*
723 *Cell & Environment* **39**: 1982–1993.

724 **Galli M, Khakhar A, Lu Z, Chen Z, Sen S, Joshi T, Nemhauser JL, Schmitz RJ, Gallavotti A.**
725 **2018.** The DNA binding landscape of the maize AUXIN RESPONSE FACTOR family. *Nature*
726 *Communications* **9**: 4526.

727 **Gómez-Ariza J, Brambilla V, Vicentini G, Landini M, Cerise M, Carrera E, Shrestha R,**
728 **Chiozzotto R, Galbiati F, Caporali E, et al. 2019.** A transcription factor coordinating internode

729 elongation and photoperiodic signals in rice. *Nature Plants* **5**: 358–362.

730 **Goretti D, Martignago D, Landini M, Brambilla V, Gómez-Ariza J, Gnesutta N, Galbiati F,**
731 **Collani S, Takagi H, Terauchi R, et al. 2017.** Transcriptional and Post-transcriptional
732 Mechanisms Limit Heading Date 1 (Hd1) Function to Adapt Rice to High Latitudes. *PLoS Genetics*
733 **13**:e1006530.

734 **Hayama R, Yokoi S, Tamaki S, Yano M, Shimamoto K. 2003.** Adaptation of photoperiodic
735 control pathways produces short-day flowering in rice. *Nature* **422**: 719–722.

736 **Itoh H, Nonoue Y, Yano M, Izawa T. 2010.** A pair of floral regulators sets critical day length for
737 Hd3a florigen expression in rice. *Nature Genetics* **42**: 635–8.

738 **Izawa T, Foster R, Chua NH. 1993.** Plant bZIP protein DNA binding specificity. *Journal of*
739 *Molecular Biology* **230**: 1131–1144.

740 **Jaeger KE, Pullen N, Lamzin S, Morris RJ, Wigge PA. 2013.** Interlocking feedback loops
741 govern the dynamic behavior of the floral transition in Arabidopsis. *The Plant Cell* **25**: 820–33.

742 **Jang S, Li H-Y, Kuo M-L. 2017.** Ectopic expression of Arabidopsis *FD* and *FD PARALOGUE* in
743 rice results in dwarfism with size reduction of spikelets. *Scientific Reports* **7**: 44477.

744 **Jung J-H, Lee H-J, Ryu JY, Park C-M. 2016.** SPL3/4/5 Integrate Developmental Aging
745 and Photoperiodic Signals into the FT-FD Module in Arabidopsis Flowering. *Molecular Plant* **9**:
746 1647–1659.

747 **Kaneko-Suzuki M, Kurihara-Ishikawa R, Okushita-Terakawa C, Kojima C, Nagano-**
748 **Fujiwara M, Ohki I, Tsuji H, Shimamoto K, Taoka KI. 2018.** TFL1-Like Proteins in Rice
749 Antagonize Rice FT-Like Protein in Inflorescence Development by Competition for Complex
750 Formation with 14-3-3 and FD. *Plant and Cell Physiology* **59**: 458–468.

751 **Kawamoto N, Sasabe M, Endo M, Machida Y, Araki T. 2015.** Calcium-dependent protein
752 kinases responsible for the phosphorylation of a bZIP transcription factor FD crucial for the florigen
753 complex formation. *Scientific Reports* **5**: 8341.

754 **Kim S-K, Park H-Y, Jang YH, Lee KC, Chung YS, Lee JH, Kim J-K. 2016.** OsNF-YC2 and
755 OsNF-YC4 proteins inhibit flowering under long-day conditions in rice. *Planta* **243**: 563–576.

756 **Kobayashi K, Maekawa M, Miyao A, Hirochika H, Kyojuka J. 2010.** *PANICLE PHYTOMER2*
757 (*PAP2*), encoding a SEPALLATA subfamily MADS-box protein, positively controls spikelet

758 meristem identity in rice. *Plant and Cell Physiology* **51**: 47–57.

759 **Kobayashi K, Yasuno N, Sato Y, Yoda M, Yamazaki R, Kimizu M, Yoshida H, Nagamura Y,**
760 **Kyozuka J. 2012.** Inflorescence meristem identity in rice is specified by overlapping functions of
761 three *API/FUL*-like MADS box genes and *PAP2*, a *SEPALLATA* MADS box gene. *The Plant Cell*
762 **24**: 1848–59.

763 **Kojima S, Takahashi Y, Kobayashi Y, Monna L, Sasaki T, Araki T, Yano M. 2002.** *Hd3a*, a
764 rice ortholog of the Arabidopsis *FT* gene, promotes transition to flowering downstream of *Hdl*
765 under short-day conditions. *Plant & Cell Physiology* **43**: 1096–105.

766 **Komiya R, Ikegami A, Tamaki S, Yokoi S, Shimamoto K. 2008.** *Hd3a* and *RFT1* are essential
767 for flowering in rice. *Development* **135**: 767–774.

768 **Komiya R, Yokoi S, Shimamoto K. 2009.** A gene network for long-day flowering activates *RFT1*
769 encoding a mobile flowering signal in rice. *Development* **136**: 3443–3450.

770 **Langmead B, Salzberg SL. 2012.** Fast gapped-read alignment with Bowtie 2. *Nature Methods* **9**:
771 357–359.

772 **Li C, Lin H, Dubcovsky J. 2015.** Factorial combinations of protein interactions generate a
773 multiplicity of florigen activation complexes in wheat and barley. *The Plant Journal* **84**: 70–82.

774 **Li D, Zhang H, Mou M, Chen Y, Xiang S, Chen L, Yu D. 2019.** Arabidopsis Class II TCP
775 Transcription Factors Integrate with the FT–FD Module to Control Flowering. *Plant Physiology*
776 **181**: 97–111.

777 **Liu Y, Cui S, Wu F, Yan S, Lin X, Du X, Chong K, Schilling S, Theißen G, Meng Z. 2013.**
778 Functional Conservation of MIKC*-Type MADS Box Genes in *Arabidopsis* and Rice Pollen
779 Maturation. *The Plant Cell* **25**: 1288–1303.

780 **Liu B, Liu Y, Wang B, Luo Q, Shi J, Gan J, Shen WH, Yu Y, Dong A. 2019.** The transcription
781 factor OsSUF4 interacts with SDG725 in promoting H3K36me3 establishment. *Nature*
782 *Communications* **10**: 1–14.

783 **Miao J, Guo D, Zhang J, Huang Q, Qin G, Zhang X, Wan J, Gu H, Qu L-J. 2013.** Targeted
784 mutagenesis in rice using CRISPR-Cas system. *Cell Research* **23**: 1233–6.

785 **Nemoto Y, Nonoue Y, Yano M, Izawa T. 2016.** *Hdl*, a *CONSTANS* ortholog in rice, functions as
786 an *Ehd1* repressor through interaction with monocot-specific CCT-domain protein Ghd7. *The Plant*

787 *Journal* **86**: 221–233.

788 **O'Malley RC, Huang S shan C, Song L, Lewsey MG, Bartlett A, Nery JR, Galli M, Gallavotti**
789 **A, Ecker JR. 2016.** Cistrome and Epicistrome Features Shape the Regulatory DNA Landscape.
790 *Cell* **166**: 1598.

791 **Oliveros J. 2007.** Venny. An interactive tool for comparing lists with Venn's diagrams. *Publicly*
792 *available at <http://bioinfogp.cnb.csic.es/tools/venny/index.html>.*

793 **Park SJ, Jiang K, Tal L, Yichie Y, Gar O, Zamir D, Eshed Y, Lippman ZB. 2014.**
794 Optimization of crop productivity in tomato using induced mutations in the florigen pathway.
795 *Nature Genetics* **46**: 1337–42.

796 **Purwestri YA, Ogaki Y, Tamaki S, Tsuji H, Shimamoto K. 2009.** The 14-3-3 protein GF14c acts
797 as a negative regulator of flowering in rice by interacting with the florigen Hd3a. *Plant and Cell*
798 *Physiology* **50**: 429–438.

799 **Sahoo KK, Tripathi AK, Pareek A, Sopory SK, Singla-Pareek SL. 2011.** An improved protocol
800 for efficient transformation and regeneration of diverse indica rice cultivars. *Plant Methods* **7**: 49.

801 **Stigliani A, Martin-Arevalillo R, Lucas J, Bessy A, Vinos-Poyo T, Mironova V, Vernoux T,**
802 **Dumas R, Parcy F. 2019.** Capturing Auxin Response Factors Syntax Using DNA Binding Models.
803 *Molecular Plant* **12**: 822–832.

804 **Supek F, Bošnjak M, Škunca N, Šmuc T. 2011.** REVIGO Summarizes and Visualizes Long Lists
805 of Gene Ontology Terms (C Gibas, Ed.). *PLoS ONE* **6**: e21800.

806 **Tamaki S, Matsuo S, Wong HL, Yokoi S, Shimamoto K. 2007.** Hd3a protein is a mobile
807 flowering signal in rice. *Science* **316**: 1033–1036.

808 **Tamaki S, Tsuji H, Matsumoto A, Fujita A, Shimatani Z, Terada R, Sakamoto T, Kurata T,**
809 **Shimamoto K. 2015.** FT-like proteins induce transposon silencing in the shoot apex during floral
810 induction in rice. *Proceedings of the National Academy of Sciences of the United States of America*
811 **112**: E901-10.

812 **Taoka K, Ohki I, Tsuji H, Furuita K, Hayashi K, Yanase T, Yamaguchi M, Nakashima C,**
813 **Purwestri YA, Tamaki S, et al. 2011.** 14-3-3 proteins act as intracellular receptors for rice Hd3a
814 florigen. *Nature* **476**: 332–5.

815 **Teo C-J, Takahashi K, Shimizu K, Shimamoto K, Taoka K. 2017.** Potato Tuber Induction is

816 Regulated by Interactions Between Components of a Tubergen Complex. *Plant and Cell*
817 *Physiology* **58**: 365–374.

818 **Tian T, Liu Y, Yan H, You Q, Yi X, Du Z, Xu W, Su Z. 2017.** agriGO v2.0: a GO analysis
819 toolkit for the agricultural community, 2017 update. *Nucleic Acids Research* **45**: W122–W129.

820 **Tsuji H, Nakamura H, Taoka K, Shimamoto K. 2013.** Functional diversification of FD
821 transcription factors in rice, components of florigen activation complexes. *Plant & Cell Physiology*
822 **54**: 385–97.

823 **Tylewicz S, Tsuji H, Miskolczi P, Petterle A, Azeez A, Jonsson K, Shimamoto K, Bhalerao RP.**
824 **2015.** Dual role of tree florigen activation complex component FD in photoperiodic growth control
825 and adaptive response pathways. *Proceedings of the National Academy of Sciences of the United*
826 *States of America* **112**: 3140–5.

827 **Wigge PA, Kim MC, Jaeger KE, Busch W, Schmid M, Lohmann JU, Weigel D. 2005.**
828 Integration of spatial and temporal information during floral induction in Arabidopsis. *Science* **309**:
829 1056–9.

830 **Wu F, Shi X, Lin X, Liu Y, Chong K, Theißen G, Meng Z. 2017.** The ABCs of flower
831 development: mutational analysis of *API/FUL*-like genes in rice provides evidence for a homeotic
832 (A)-function in grasses. *The Plant Journal* **89**: 310–324.

833 **Xue W, Xing Y, Weng X, Zhao Y, Tang W, Wang L, Zhou H, Yu S, Xu C, Li X, et al. 2008.**
834 Natural variation in *Ghd7* is an important regulator of heading date and yield potential in rice.
835 *Nature Genetics* **40**: 761–767.

836 **Yano M, Katayose Y, Ashikari M, Yamanouchi U, Monna L, Fuse T, Baba T, Yamamoto K,**
837 **Umehara Y, Nagamura Y, et al. 2000.** *Hdl*, a major photoperiod sensitivity quantitative trait locus
838 in rice, is closely related to the Arabidopsis flowering time gene *CONSTANS*. *The Plant Cell* **12**:
839 2473–2484.

840 **ZHANG S, WANG S, XU Y, YU C, SHEN C, QIAN Q, GEISLER M, JIANG DA, QI Y. 2015.**
841 The auxin response factor, OsARF19, controls rice leaf angles through positively regulating *OsGH*
842 *3-5* and *OsBRI 1*. *Plant, Cell & Environment* **38**: 638–654.

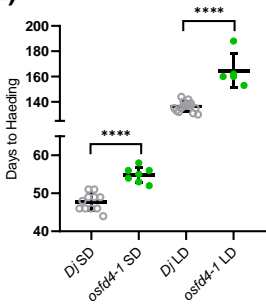
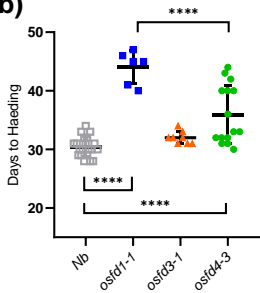
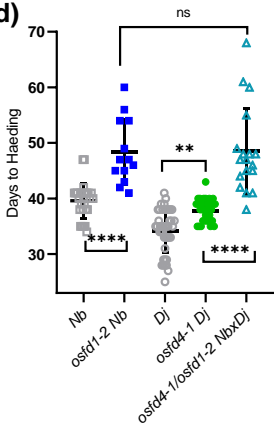
843 **Zhao J, Chen H, Ren D, Tang H, Qiu R, Feng J, Long Y, Niu B, Chen D, Zhong T, et al. 2015.**
844 Genetic interactions between diverged alleles of *Early heading date 1 (Ehd1)* and *Heading date 3a*
845 (*Hd3a*)/*RICE FLOWERING LOCUS T1 (RFT1)* control differential heading and contribute to

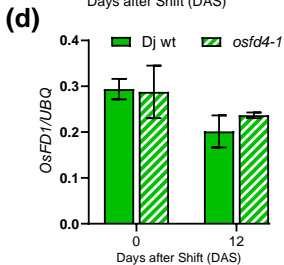
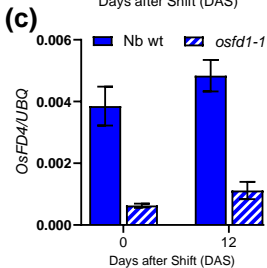
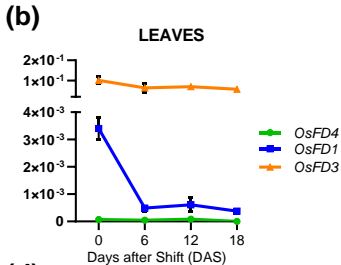
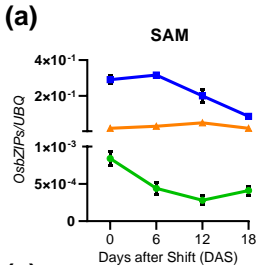
846 regional adaptation in rice (*Oryza sativa*). *New Phytologist* **208**: 936–948.

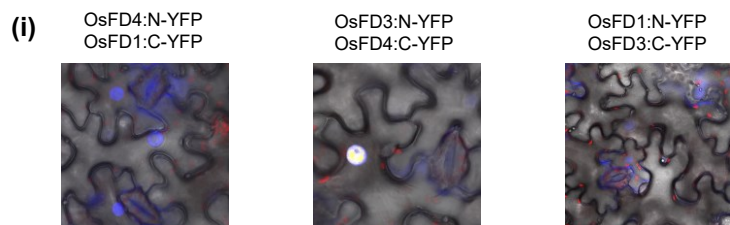
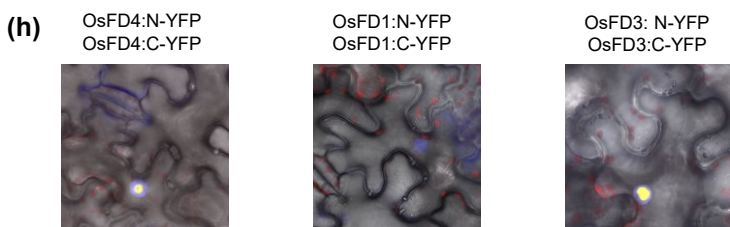
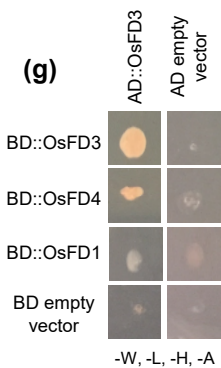
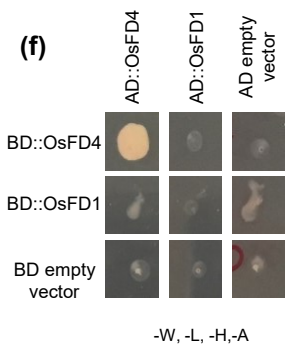
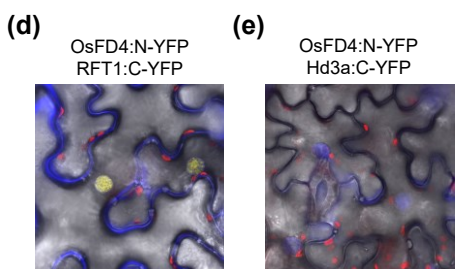
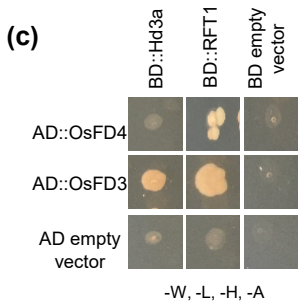
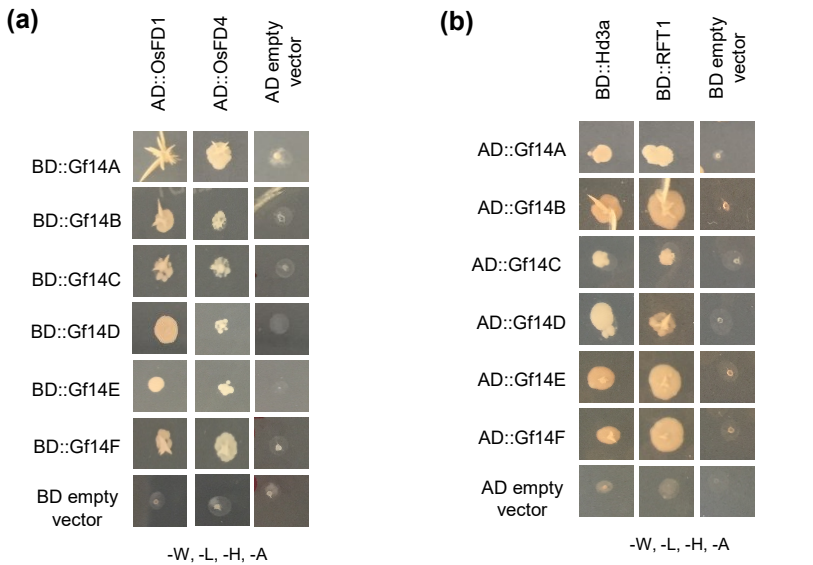
847 **Zhu S, Wang J, Cai M, Zhang H, Wu F, Xu Y, Li C, Cheng Z, Zhang X, Guo X, et al. 2017.**

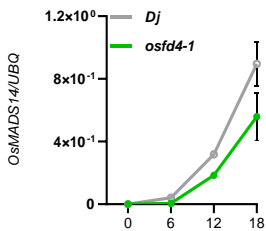
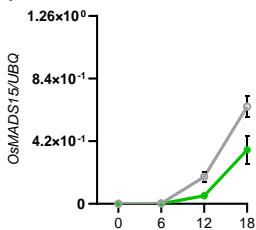
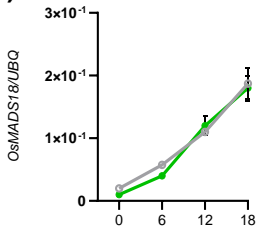
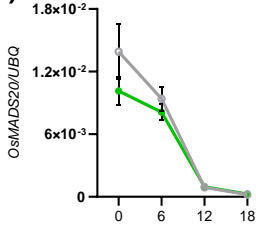
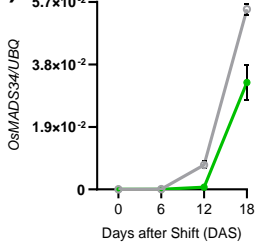
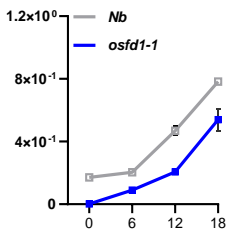
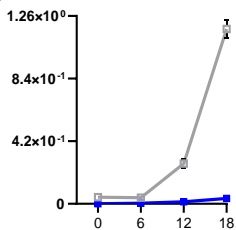
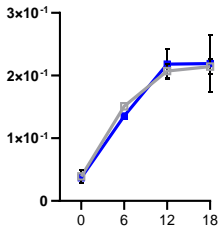
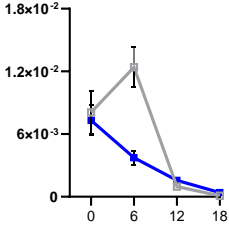
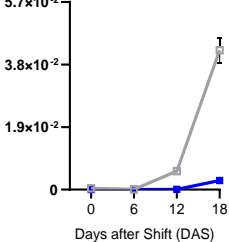
848 The OsHAPL1-DTH8-Hd1 complex functions as the transcription regulator to repress heading date

849 in rice. *Journal of Experimental Botany* **68**: 553–568.

(a)**(b)****(c)****(d)**

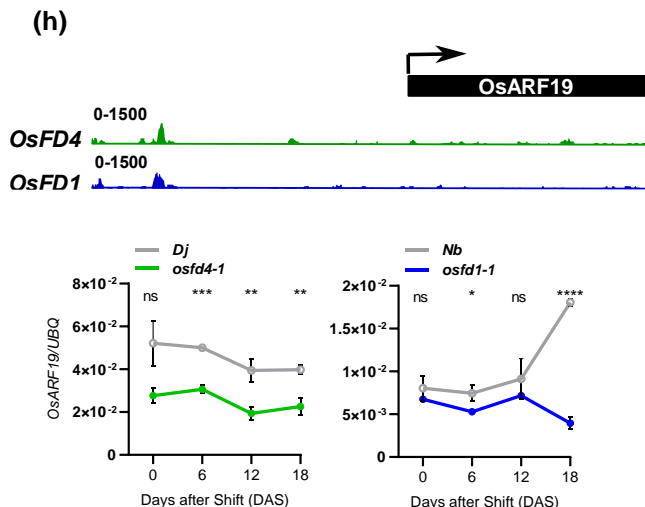
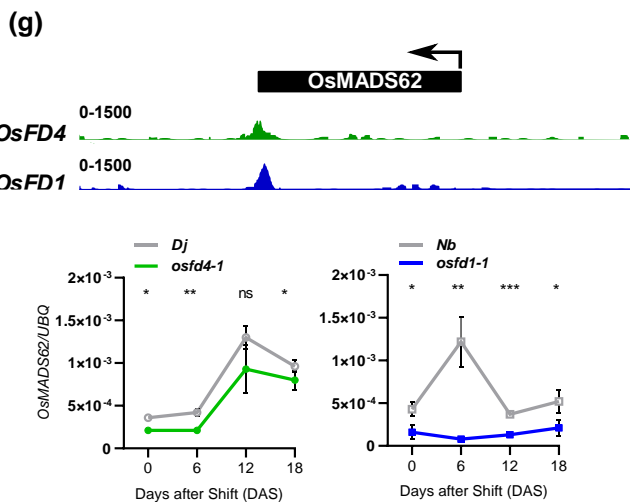
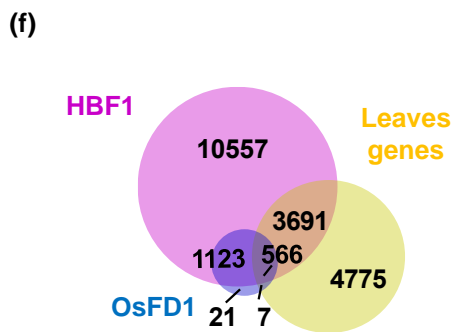
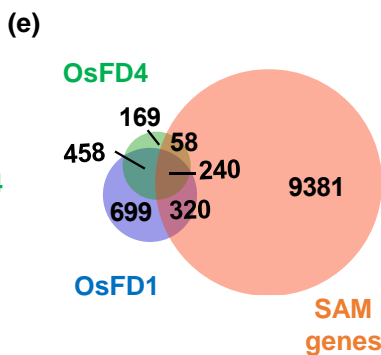
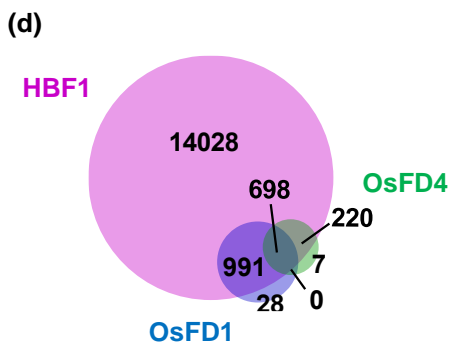
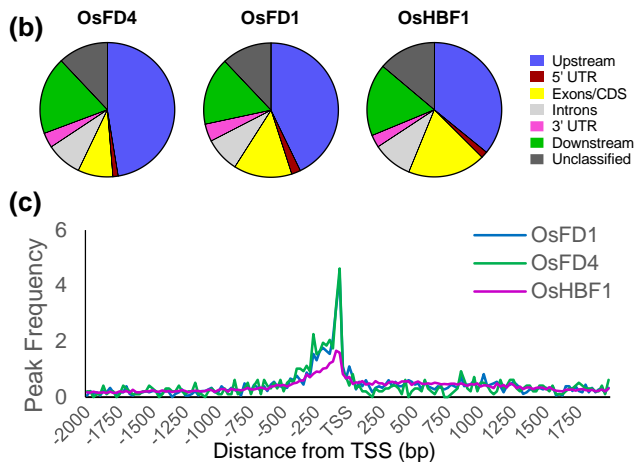


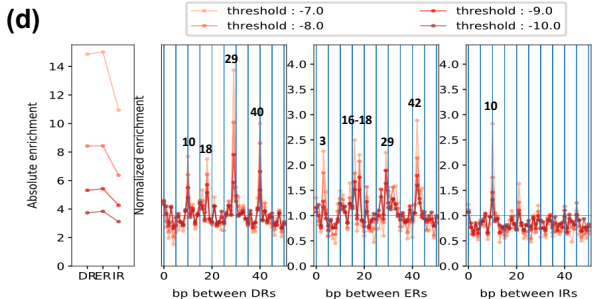
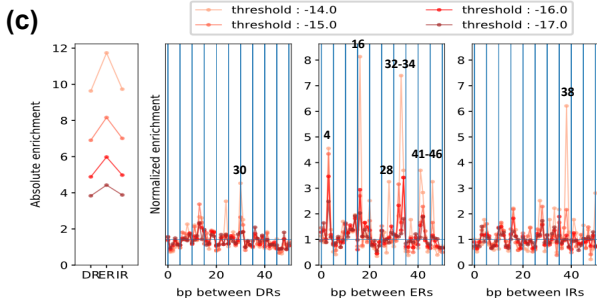
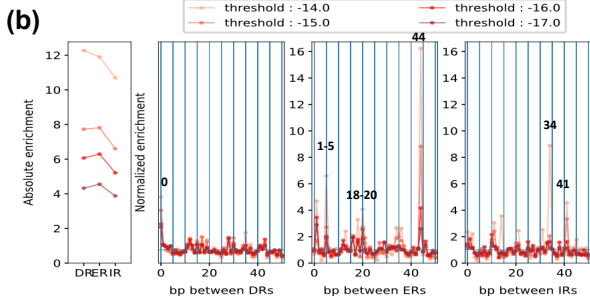
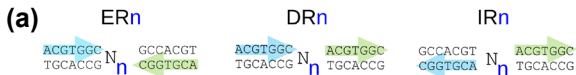


(a)**(b)****(c)****(d)****(e)****(f)****(g)****(h)****(i)****(j)**

(a)

bZIP	Nr of peaks	Nr of putative target genes	Motif
HBF1	28323	15937	
OsFD1	2059	1717	
OsFD4	1107	925	





New Phytologist Supporting Information

Article title: OsFD4 promotes the rice floral transition via Florigen Activation Complex formation in the shoot apical meristem

Authors: Martina Cerise, Francesca Giaume, Mary Galli, Bahman Khahani, Jérémy Lucas, Federico Podico, Elahe Tavakol, François Parcy, Andrea Gallavotti, Vittoria Brambilla and Fabio Fornara

Article acceptance date: 15 July 2020

The following Supporting Information is available for this article:

Fig. S1 Genotype and phenotype of *OsFD4* and *OsFD1* mutants

Fig. S2 OsFD3 and Gf14s Y2H assays and OsFD4-Hd3a BiFC

Fig. S3 Y2H mating controls

Fig. S4 Venn diagram showing the overlap between targets of AtFD, OsFD1, OsFD4 and HBF1

Fig. S5 Expression analysis of some DAP-seq targets in *osfd4-1* and *osfd1-1*

Fig. S6 Spacing analysis control: OsFD4, OsFD1 and HBF1 ROC curves

Table S1 Sequences of oligonucleotides used in this study

Table S2 Arabidopsis orthologs of rice genes (see separate file)

Table S3 List of OsFD4, OsFD1 and HBF1 DAP-seq bound genes (see separate file)

Table S4 List of genes shown in Figure S4 (see separate file)

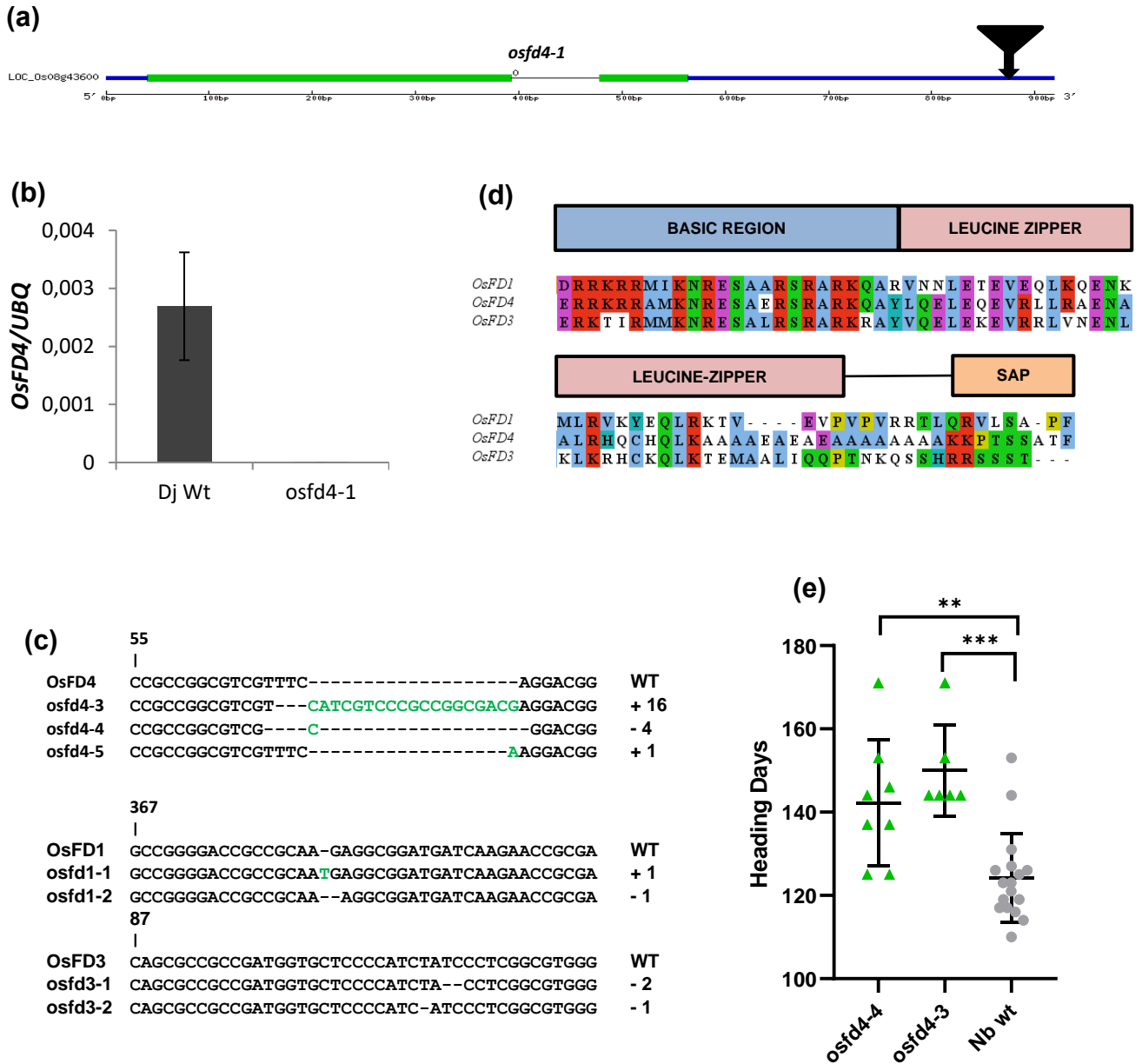


Fig. S1 (a) Map of the *osfd4-1* mutant locus. Green and blue lines represent exons and UTR regions, respectively. A black line indicates an intron. A triangle in the 3'UTR region indicates the position of the T-DNA insert. (b) Expression of *OsFD4* in the SAM of Dj wild type and *osfd4-1* mutant. Data are average \pm StDev of three technical replicates. (c) Sequences of mutant alleles of *osfd4*, *osfd1* and *osfd3* obtained using CRISPR. Inserted nucleotides are indicated in green. (d) Protein alignment of the C-terminus region of OsFD1, OsFD4 and OsFD3 starting from the basic leucine zipper domain. (e) Flowering time under LD conditions of *osfd4-3* and *osfd4-4*.

Data are represented as mean \pm StDev. Asterisks indicate the p-value calculated using ANOVA, ***= $p < 0.001$, **= $p < 0.01$.

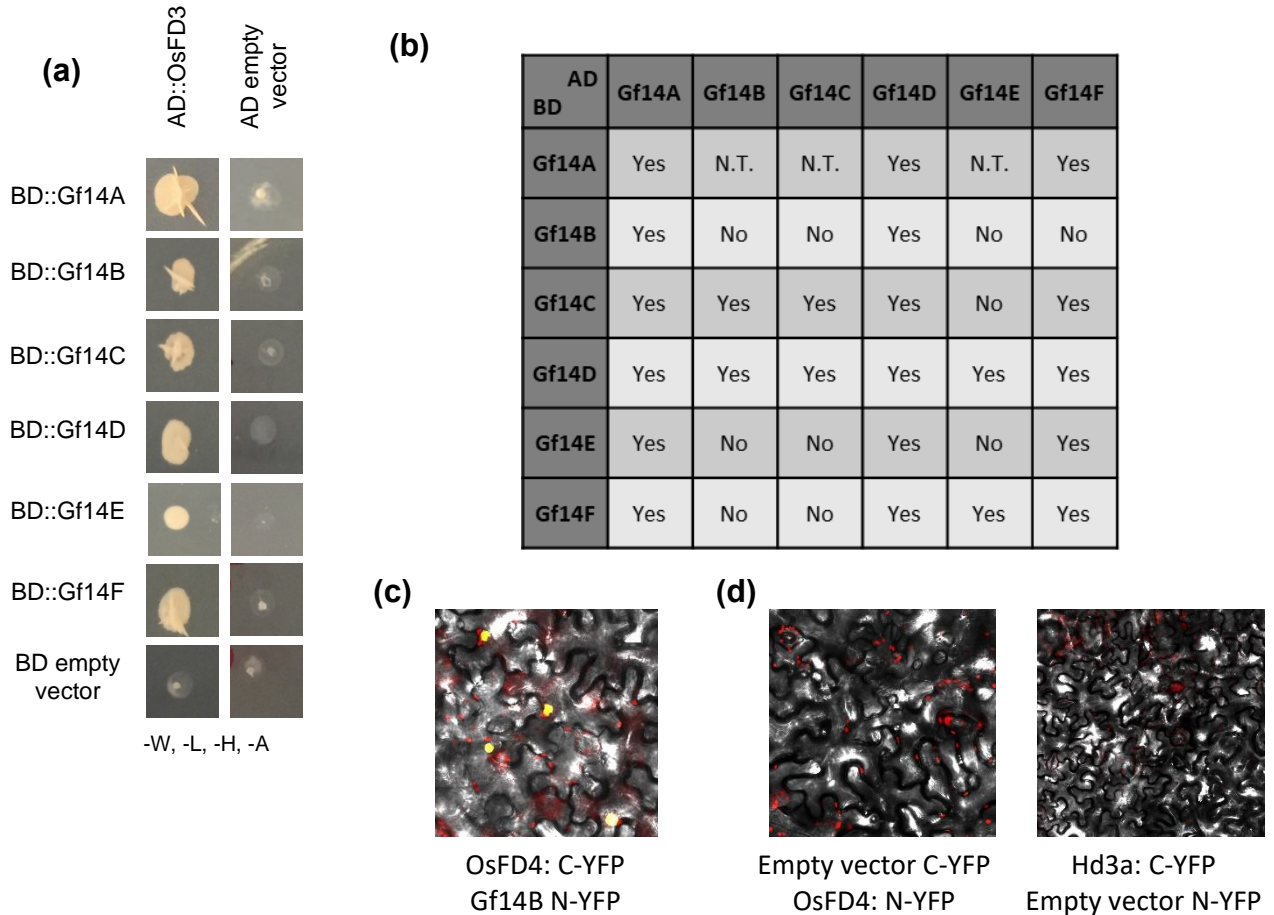


Fig. S2 (a) Yeast two Hybrid (Y2H) among Gf14A-F fused to the Binding Domain (BD) and OsFD3 fused to the Activation Domain (AD). (b) Double entry table summarizing homo- and heterodimerizations among Gf14A-F. Interactions were assessed on drop out media lacking L, W, H and A. N.T., not tested. (c) Bimolecular fluorescence complementation (BiFC) between OsFD4 fused with C-terminus of YFP (C-YFP) and Gf14B fused with the N-terminus of YFP (N-YFP). (d) BiFC between empty C-YFP vector and OsFD4 fused with N-YFP (left); Hd3a fused with C-YFP and N-YFP empty vector (right). Negative controls were done for every independent BiFC assay performed; here representative ones are shown.

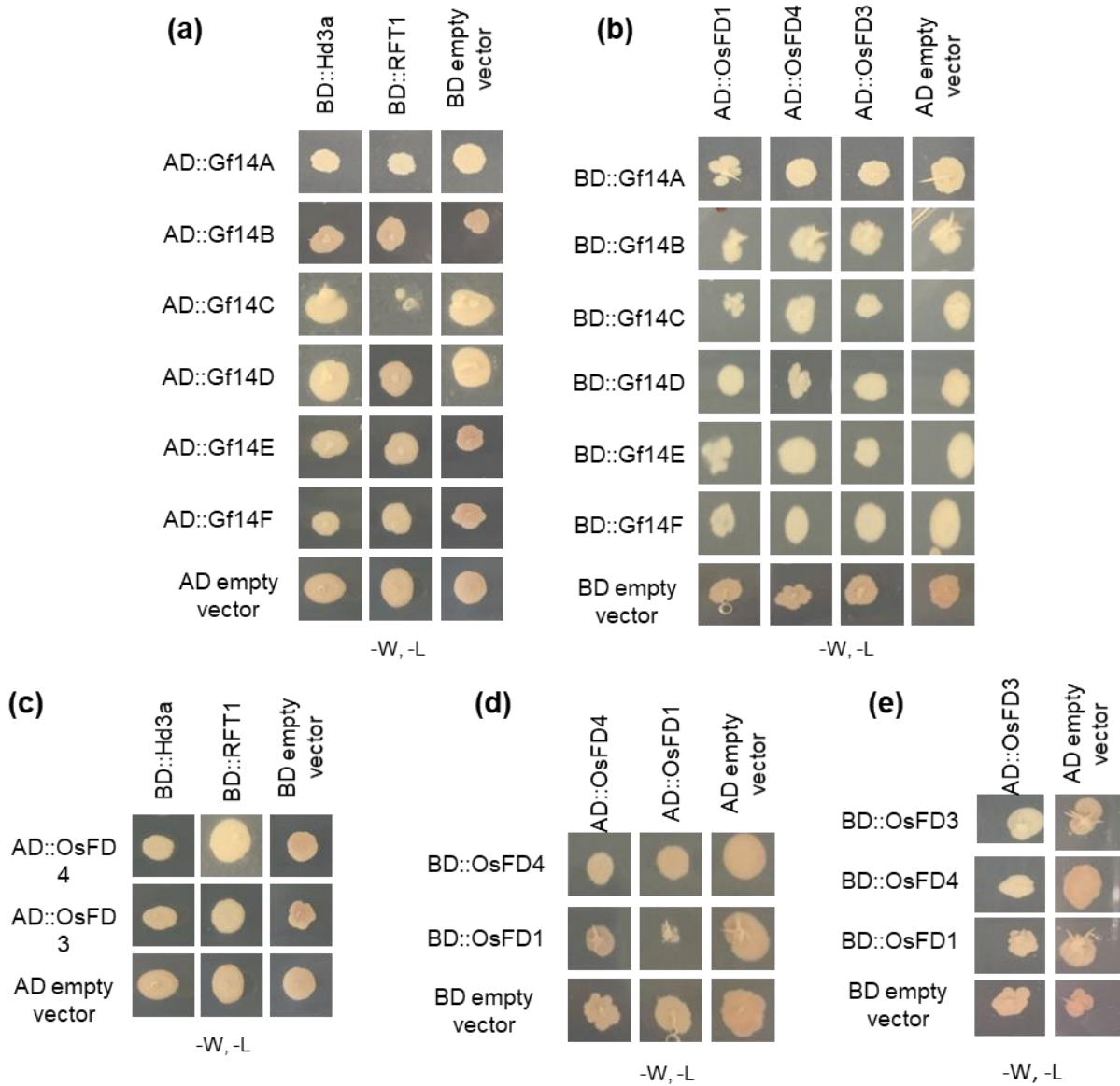


Fig. S3 (a) Mating controls of the Y2H among Gf14A-F fused to the AD and Hd3a or RFT1 fused to the BD. (b) Mating controls of the Y2H among Gf14A-F fused to the BD and OsFD1, OsFD4 and OsFD3 fused to the AD. (c) Mating controls of the Y2H among OsFD4 and OsFD3 fused to the AD and Hd3a and RFT1 fused to the BD. (d) Mating controls of the Y2H among OsFD4 and OsFD1 fused with the AD or the BD. (e) Mating controls of the Y2H among OsFD3, OsFD4 and OsFD1 fused to the BD and OsFD3 fused to the AD. All controls were grown on yeast medium lacking W and L.

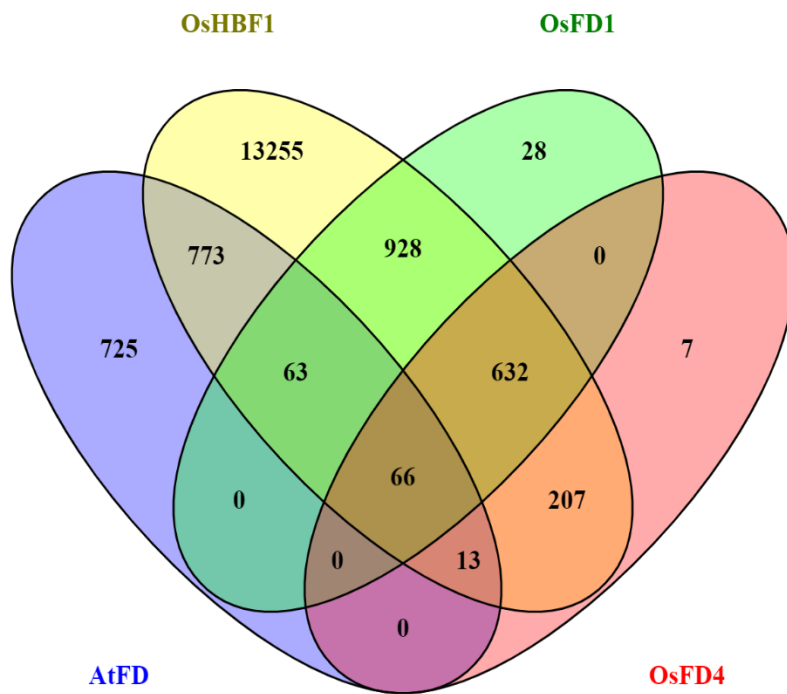


Fig. S4 Venn diagram showing the overlap between targets of AtFD, OsFD1, OsFD4 and HBF1.

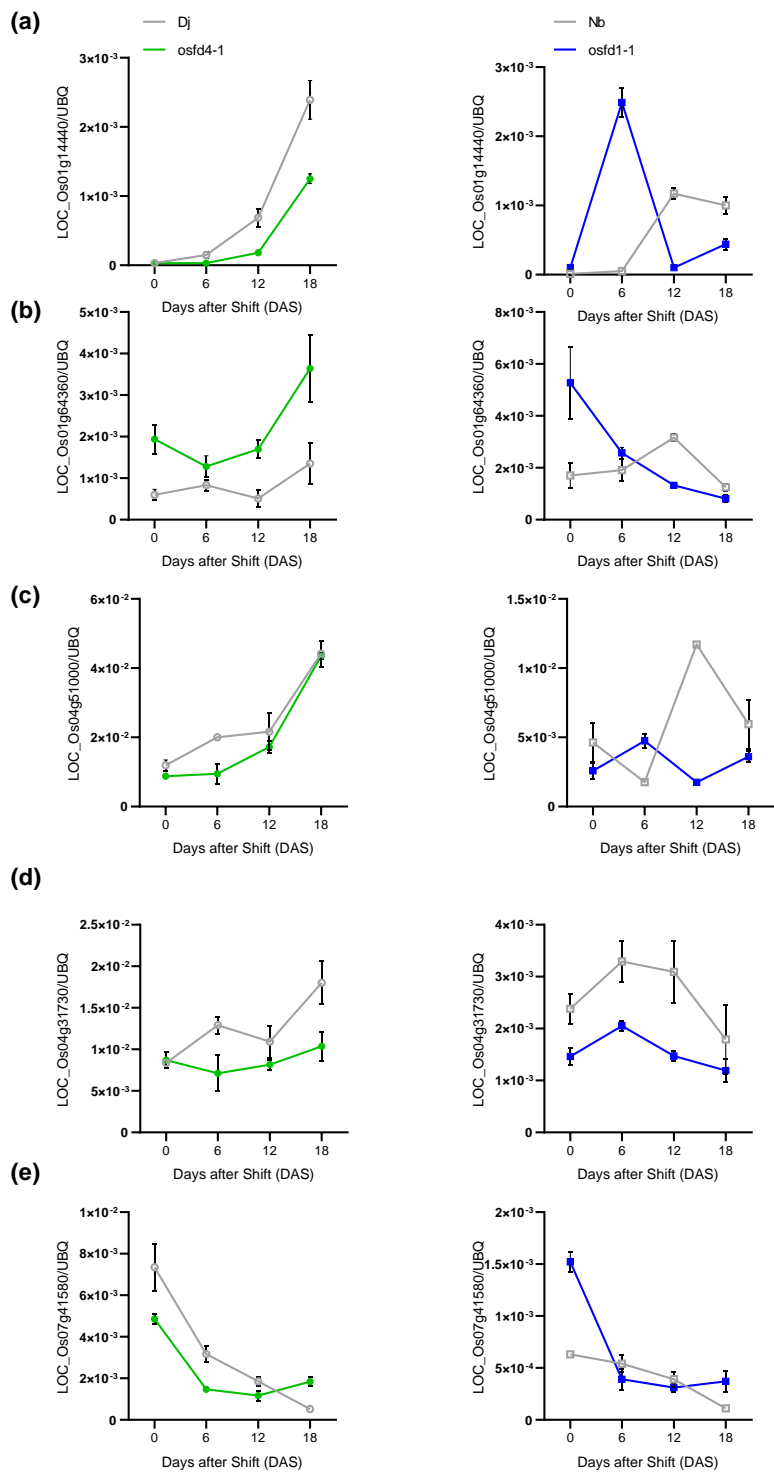


Fig. S5 Quantification of transcripts of LOC_Os01g14440 (WRKY) (a), LOC_Os01g64360 (MYB) (b), LOC_Os04g51000 (RICE FLORICAULA/LEAFY) (c), LOC_Os04g31730 (B3) (d) and

LOC_Os07g41580 (NF-YB) (e) in *osfd4-1* and *osfd1-1* mutants. Data are represented as mean \pm StDev.

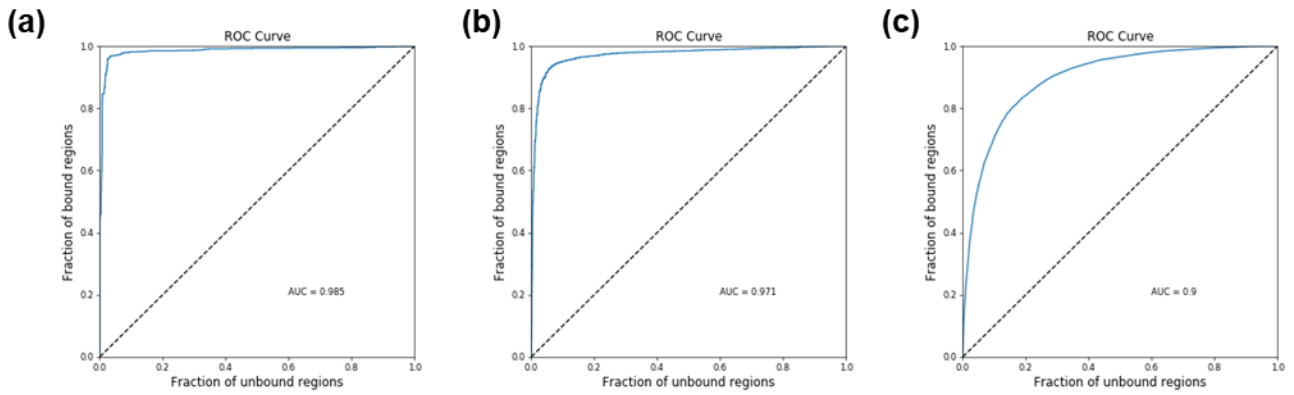


Fig. S6 Receiver Operating Characteristics (ROC) analysis of OsFD4 (a), OsFD1 (b) and HBF1 (c) estimating the prediction power of Position Weight Matrices (PWMs), i.e. the capability of OsbZIPs binding sites to differentiate between bound and not bound regions. AUC, Area Under the Curve.

Table S1 Sequences of oligonucleotides used in this study.

Number	Sequence	Gene
Os_892	GACAACGTGAAGGCGAAGA	UBQ Fw for qRT-PCR
Os_893	CACCAGGTGGAGTGTGGAC	UBQ Rv for qRT-PCR
Os_245	CCGGGCTATGGAGTGAAAT	OsFD4 Fw for qRT-PCR
Os_246	TGCTCTCATATTCTCCATGCTG	OsFD4 Rv for qRT-PCR
Os_160	TTCAGGTGGACGACCTTAGC	OsFD1 Fw for qRT-PCR
Os_161	GCTAGCAGCTGCCAACACT	OsFD1 Rv for qRT-PCR
Os_158	CGGTTGCGAGACGAGGAA	OsMADS14 Fw for qRT-PCR
Os_159	GAAAGACGGTGCTGGACGAA	OsMADS14 Rv for qRT-PCR
Os_239	CGTCGTCGGCCAAAACAG	OsMADS15 Fw for qRT-PCR
Os_240	TGACTTCAATTCATTCAAGGTTGCT	OsMADS15 Rv for qRT-PCR
Os_353	TGTTCTGCAAAAGCTCATGG	OsMADS18 Fw for qRT-PCR
Os_354	TTGGTGATGATGTGCTTGGT	OsMADS18 Rv for qRT-PCR
Os_1353	GCTCCAGTCATCATCGAACG	OsMADS20 Fw for qRT-PCR
Os_1354	GGAGATACTACTACCGCTCACT	OsMADS20 Rv for qRT-PCR
Os_186	TTGATGAACTTGCGACCTAAA	OsMADS34 Fw for qRT-PCR
Os_187	TGCTGCAGTTTCCGTTCC	OsMADS34 Rv for qRT-PCR
Os_1312	AGAGGGGCAACTTGAGGAAC	OsARF19 Fw for qRT-PCR
Os_1313	GCAACCGACAAATTCCTCC	OsARF19 Rv for qRT-PCR
Os_1341	CAGTACCTGTGATGGAGCA	OsMADS62 Fw for qRT-PCR
Os_1342	GTTGCTGTGCTACGCCATG	OsMADS62 Rv for qRT-PCR
Os_1349	GCAACACCAACAACAAGC	LOC_Os01g14440 Fw for qRT-PCR
Os_1350	AGTGTATACCATGTGCCACT	LOC_Os01g14440 Rv for qRT-PCR
Os_1351	GCATCCATGACATCACCACC	LOC_Os01g64360 Fw for qRT-PCR
Os_1352	ATCAGAGAGCCCAAGTGAC	LOC_Os01g64360 Rv for qRT-PCR
Os_1369	GTTCAGGGTGCAGGTCCTC	LOC_Os04g31730 Fw for qRT-PCR
Os_1370	ACCTGAAACTGAAACCTCCCA	LOC_Os04g31730 Rv for qRT-PCR
Os_1371	ATGGTGATGGGAGGGAAAGG	LOC_Os07g41580 Fw for qRT-PCR
Os_1372	ACCCGACATGTCCTCTGATT	LOC_Os07g41580 Rv for qRT-PCR
Os_1373	GTACGTGCCACCAGACT	LOC_Os04g51000 Fw for qRT-PCR
Os_1374	GCCCAACACCACAGGAAAC	LOC_Os04g51000 Rv for qRT-PCR
Os_1151	GGCACCGCCGGCGTCGTTTCAGGA	Oligo CRISPR OsFD4 Fw
Os_1152	AAACTCCTGAAACGACGCCGGCGG	Oligo CRISPR OsFD4 Rv
Os_936	GGCATCTTGATCATCCGCCTTTG	Oligo CRISPR OsFD1 Fw
Os_937	AAACCAAGAGGCGGATGATCAAGA	Oligo CRISPR OsFD1 Rv
Os_1153	GGCAGCCCACGCCGAGGGATAGAT	Oligo CRISPR OsFD3 Fw
Os_1154	AAACATCTATCCCTCGGCGTGGGC	Oligo CRISPR OsFD3 Rv